



HAL
open science

Sizable pool of labile organic carbon in peat and mineral soils of permafrost peatlands, western Siberia

Artem Lim, Sergey Loiko, Oleg Pokrovsky

► To cite this version:

Artem Lim, Sergey Loiko, Oleg Pokrovsky. Sizable pool of labile organic carbon in peat and mineral soils of permafrost peatlands, western Siberia. *Geoderma*, 2022, 409, pp.115601. 10.1016/j.geoderma.2021.115601 . hal-04842469

HAL Id: hal-04842469

<https://ut3-toulouseinp.hal.science/hal-04842469v1>

Submitted on 18 Dec 2024

HAL is a multi-disciplinary open access archive for the deposit and dissemination of scientific research documents, whether they are published or not. The documents may come from teaching and research institutions in France or abroad, or from public or private research centers.

L'archive ouverte pluridisciplinaire **HAL**, est destinée au dépôt et à la diffusion de documents scientifiques de niveau recherche, publiés ou non, émanant des établissements d'enseignement et de recherche français ou étrangers, des laboratoires publics ou privés.



Distributed under a Creative Commons Attribution 4.0 International License

1
2 **Sizable pool of labile organic carbon in peat and mineral soils**
3 **of permafrost peatlands, western Siberia**

4
5
6 Artem G. Lim¹, Sergey V. Loiko¹, Oleg S. Pokrovsky^{2,3*}

7
8 ¹ *BIO-GEO-CLIM Laboratory, Tomsk State University, Lenina Pr. 35, 634050, Tomsk, Russia*

9 ² *Geoscience and Environment Toulouse, UMR 5563 CNRS, University of Toulouse, 14 Avenue Edouard*
10 *Belin, 31400, Toulouse, France*

11 ³ *Institute of Ecological Problems of the North, N. Laverov Federal Center for Integrated Arctic Research,*
12 *Nab. Severnoi Dviny 23, 163000, Arkhangelsk, Russia*

13
14 Submitted to *Geoderma*, after revision November 2021

15
16
17 Key words: carbon, adsorption, mineral, soil, permafrost, experiment

29 Abstract

30 In contrast to good knowledge of dissolved organic matter (DOM) adsorption on mineral soils in
31 temperate climate, the behavior of DOM in frozen mineral horizons located under peat soils of permafrost-
32 affected regions remains poorly characterized. Yet, these regions contain sizeable and potentially highly
33 labile pools of organic (peat) carbon (C) that may migrate downwards across mineral layers in case of
34 massive thaw in frozen peatlands induced by on-going climate warming. To quantify these pools and the
35 lability of DOM in permafrost peat soils, we performed experiments focusing on dissolved organic carbon
36 (DOC) desorption from, and adsorption onto, mineral horizons (iron-poor and iron-rich sands as well as silt
37 loam) from the largest frozen peatland in the world, the western Siberia Lowland (WSL). Desorbed DOC
38 ranged between 0.1 and 0.6 mg C g_{soil}⁻¹ depending on type of mineral substrate. The adsorption of peat
39 leachate DOM ranged between 0.1 and 0.5 mg C g_{soil}⁻¹ being highest in Al-Fe-rich mineral horizons.

40 Field measurements of C pools in peat and underlying mineral horizons over 1 m depth in the
41 discontinuous permafrost zone yielded 47 and 15 kg C m⁻², respectively. The organic carbon (OC)
42 adsorption capacity of the 1 m - thick mineral layers represented < 2% of total amount of OC containing in
43 the 1 m - thick peat layer. However, this adsorption capacity is comparable to the amount of DOC that can
44 be leached from overlaying peat horizons (18 %). On average, out of 1.38±0.13 kg C m⁻² capable of being
45 initially released from the upper 0-100 cm of peat, 0.25±0.19 kg C m⁻² can be adsorbed by the underlying
46 100-200 cm of Fe- and Al-rich sands and clays. The remaining 1.13 kg C m⁻² can be exported to lakes and
47 rivers. Therefore, DOC released during peat thaw in upper soil horizons in permafrost regions can be sizably
48 attenuated via adsorption on mineral layers. This should be taken into account when modeling the feedback
49 of permafrost thaw on C export and CO₂ emissions.

54 1. Introduction

55 The fate of organic carbon (OC) stored in peat and mineral frozen deposits of the Northern
56 Hemisphere under climate warming and permafrost thaw scenario is a central issue in modern Earth surface
57 biogeochemistry (Feng et al., 2013; Kramer and Chadwick, 2018; Ciais et al., 2019; Opfergelt, 2020).
58 Global C storage in peatlands is 530 ± 160 Pg C, and 80 % of this storage occurs in northern peatlands
59 (Hugelius et al., 2020). The western Siberian Lowland (WSL) contains a vast amount of carbon (70 Pg,
60 Sheng et al., 2004) in the form of massive 1-3 m thick peat deposits, most of which are currently frozen
61 (Kremenetski et al., 2003; Smith et al., 2004). The frozen peat in the WSL is highly vulnerable to thawing;
62 permafrost temperatures in these regions are close to zero and zones of sporadic to discontinuous, rather than
63 continuous, permafrost prevail (Romanovsky et al., 2010). As a result, a sizeable proportion of OC stored in
64 this peat can be exchanged with the hydrological network and the atmosphere. There are two main pathways
65 of OC removal from the soil system. A part of OC is dissolved via peat leaching by soil water and removal
66 to the surface waters, whereas another part can be mineralized by bacteria and emitted into the atmosphere
67 (Schuur et al., 2008, 2009; Gentsch et al., 2015a; Serikova et al., 2018, 2019). However, frozen mineral
68 horizons, which underlay peat layers, can act as important sinks of OC due to their high affinity to DOC (Gu
69 et al., 1994; Kaiser, 1998; Kalbitz et al., 2005; Kothawala et al., 2012). For example, in the south of western
70 Siberia, these mineral soils are known to decrease lateral export of DOM: the catchments of southern rivers
71 exhibit extended unfrozen mineral horizons compared to those of northern rivers because the latter drain
72 essentially frozen peat (Frey and McClelland, 2009; Kawahigashi et al., 2004; Pokrovsky et al., 2015). This
73 mechanism of surface DOM retention by deep horizons of mineral soil is thought to be of importance for
74 high latitude and boreal regions (Kaiser and Guggenberger, 2000) without an impermeable permafrost table,
75 where infiltration of organic-rich surface waters to deep mineral layers and DOC sorption on clay minerals
76 may occur causing a decrease the overall DOC export (Smedberg et al., 2006).

77 A number of factors are known to govern DOC retention in mineral soils [typically B horizon of
78 podzols as noted by Zysset and Berggren (2001)] such as: 1) adsorption onto Al and Fe sesquioxides (Kaiser
79 et al., 1996; Kaiser and Zech, 1998; Kleber et al., 2005; Kothawala et al., 2009; Moore et al., 1992;
80 Pengerud et al., 2014), and 2) co-precipitation of DOM with Al and Fe oxy(hydr)oxides (Buurman, 1985;
81 Kaiser, 1998; Nierop et al., 2002; Mu et al., 2016) and 3) DOM retention onto other mineral phases (i.e.,

82 clay minerals, Mn oxides, Zysset and Berggren, 2001; Jardin et al., 1989; Oosterwoud et al., 2010). In
83 contrast to numerous works demonstrating a dominating role of mineral surfaces in DOM transport in non-
84 permafrost soils (i.e. Groeneveld et al., 2020; Kaiser et al., 1996; Kaiser and Guggenberger, 2000;
85 Kothawala et al., 2009; Porras et al., 2017; Ussiri and Johnson, 2004)), limited information is available on
86 transport of DOM between organic (i.e., peat) and mineral (sand, clay) horizons in permafrost-affected soils.
87 In the latter settings, the underlying DOC-poor mineral horizons can be separated from organic-rich upper
88 soil/peat layers via an impermeable permafrost boundary. As a result, the water and OM residence time and
89 DOM bioavailability/biodegradation potential in the mineral soil horizons of the permafrost zone can be
90 drastically different from those of the non-permafrost zone, and even autochthonous subducted OM can be
91 protected from decomposition via, for example, cryoturbation (i.e., Čapek et al., 2015).

92 A few experimental studies of DOC adsorption on the mineral fraction of soils in arctic and subarctic
93 regions provided experimental parameters of DOC retention by mineral layers in the non-peat context
94 (Dahlgren and Marrett, 1991; Kothawala et al., 2009; Pengerud et al., 2014). In these works, the authors
95 performed laboratory assessment of adsorption constants, partitioning coefficients and reactive soil pool of C
96 for a large number of mineral horizons. Several other studies demonstrated the importance of organo-
97 mineral (Prater et al., 2020), and organo-ferric (Patzner et al., 2020) associations and bioavailability of
98 mineral-associated organic matter in permafrost soils (Gentsch et al., 2015b). Of special note is a work on
99 the role of soil clay fraction in DOM sorption across the forest-tundra gradient in Central Siberia
100 (Kawahigashi et al., 2006). These authors demonstrated that large concentrations of DOM comprising large
101 shares of hydrophilic fraction can pass mineral soils where the active layer is thin (such as Gelisols), and
102 enter streams, whereas soils with deep active layer such as inceptisols release little DOM because of DOM
103 adsorption onto their thick mineral horizons. Furthermore, Prokushkin et al. (2007) related the DOM
104 adsorption capacity of the mineral soils to the lateral export/retention of DOM by rivers across the gradient
105 of active layer thickness in the non-peatland soils of the Yenisey basin in Central Siberia and demonstrated
106 that DOM produced in the active layer is retained and stabilized in underlying, unfrozen mineral soils.
107 Sizable retention of DOM on unfrozen mineral horizons was later confirmed by quantitative estimations of
108 DOM release from frozen peat layers and impact of DOM adsorption capacity by mineral horizons on DOM

109 export fluxes in rivers of western Siberia, draining through partially frozen peat deposits (Pokrovsky et al.,
110 2015). However, quantification of parameters controlling DOM adsorption onto and release from frozen
111 mineral horizons and quantitative estimation of reaction parameters in the peatland context remains very
112 limited. A lack of this information precludes the predictive assessment of the link between the permafrost
113 thaw (deepening of the active layer) and C emission and export in frozen peatlands of arctic and subarctic
114 regions via quantitative modeling at the catchment scale (i.e., Jantze et al., 2013; Tang et al., 2018).

115 To bridge this knowledge gap, we estimated the soil organic carbon (SOC) pool in organic and
116 mineral layers in both thawed and frozen horizons in typical soil environments of the permafrost peatlands in
117 the western Siberia Lowland (WSL). We further performed laboratory experiments on DOC release from
118 peat and adsorption onto various mineral soils that were sampled in permafrost peatlands of the region. Our
119 experimentation goal was to answer 3 specific questions: 1) How much DOC issued from frozen peat can be
120 retained by mineral horizons during thaw of peatlands? 2) Is there a strong control of Al- and Fe-oxides on
121 DOC adsorption by mineral soils (as known for non-permafrost environments)? and 3) Is the magnitude of
122 DOC cycling between organic and mineral horizons at the watershed scale comparable with lateral export of
123 C from watershed soils? It is anticipated that, when combined with natural observations of SOC pools in
124 peat and mineral horizons as well as with DOC riverine fluxes, these experimental results will allow possible
125 prediction of changes in soil C stocks and fluxes that are induced by thawing of organic (peat) horizons and
126 transport of DOC over the mineral layers.

128 **2. Materials and methods**

129 *2.1. Site description and soil sampling*

130 Peat core samples were collected in the northern part of west Siberian Lowland at the Khanymey
131 INTERACT station (<https://eu-interact.org/>) in the discontinuous permafrost zone (forest-bog biome) and at
132 the Tazovsky site in the continuous permafrost zone (polygonal tundra), **Fig. 1 and S1**. A detailed
133 description of the sites is provided elsewhere (Loiko et al., 2019; Morgalev et al., 2017; Raudina et al., 2018,
134 2017). Peat and mineral horizons were sampled in the end of August 2017 when the active layer thickness
135 (ALT) was at maximum. The peat (0.4-1.5 m thick on Khanymey) developed on sands with minor amounts

136 of clay and silt. The dominant soil catenae are flat-mound bogs along the watershed divides which comprise
137 the Hemic Cryic Histosols on mounds (palsas) and Fibric Gelic Histosols on fens. The soil specifications
138 from here forward are termed according to WRB IUSS (2015). Average active layer thickness is 41 ± 5 cm at
139 the top of mounds and between 1 and 2 m in depressions and hollows. For experiments described below, we
140 collected the frozen peat from the peat mound and three types of sandy soil horizons (0.05-0.50 mm grain
141 size) underlying peat deposits (E, Bs and Bh horizons). The mineral layers had C content from 1.4 to 40 mg
142 g^{-1} and Fe content from 0.4 to 3.1 mg g^{-1} (**Table 1**). Typical soil profiles containing thawed and frozen peat
143 and frozen mineral deposits from the discontinuous permafrost zone collected for leaching and adsorption
144 experiments are shown in **Fig. 1**.

145 The second sampling site was located in the continuous permafrost zone, near town of Tazovsky,
146 where polygonal tundra developed on thick (2-4 m) peat deposits underlain by silt/loam mineral deposits.
147 Note that in the continuous permafrost zone (Tazovsky), we collected only frozen silt loam material (a
148 mixture of < 0.05 and < 0.002 mm grain size underlying a 4 m-thick frozen peat) because such type of
149 substrate is absent in Khanymey.

150 Core samples of frozen peat and mineral deposits were extracted using a motorized Russian peat
151 corer (UKB-12/25 I, Russia) with a 4-cm diameter corer sterilized with 40% ethanol prior to each extraction.
152 Thawed horizons were sampled laterally at discrete depths from a 1 x 1 m pit using a ceramic knife. The
153 lateral stock of organic carbon in peat and underlying mineral deposits was estimated in the discontinuous
154 permafrost zone, where we disposed 11 independent cores (7 to 15 horizons in each core), sampled from
155 positive (mounds) and negative (hollows, depressions) micro-landscapes (**Table S1**). In order to evaluate the
156 lateral storage of C in peat and mineral horizons, each 5 cm of both peat and mineral horizons of the drilled
157 core were collected using a clean ceramic knife and stored frozen at $-18^{\circ}C$ before freeze-drying in the
158 laboratory. The density and C concentration were measured on bulk sample with a resolution of 5 cm.

159 160 *2.2. DOC leaching from peat*

161 Peat leachate was prepared using the frozen peat horizon (55-75 cm), which was sampled below the
162 bottom boundary of the active layer (~ 40 cm) of the frozen mound in the discontinuous permafrost site

(Khanymey). The frozen peat was reacted at $10 \text{ g}_{\text{dry peat}} \text{ L}^{-1}$ with Milli-Q water in a sterile glass bottle under gentle stirring over 24 h at room temperature. The obtained solution was filtered through a sterile Sartorius filtration unit ($0.22 \text{ }\mu\text{m}$) and stored in the refrigerator prior to adsorption experiments.

The capacity of frozen peat to release DOC was studied by varying the concentration of peat in Milli-Q water (1, 2, 5, 10, 20 and $100 \text{ g}_{\text{peat}} \text{ L}^{-1}$) placed in 60-mL aerobic glass reactors and measuring the resulting DOC concentration ($< 0.45 \text{ }\mu\text{m}$) at the steady-state (pseudo-equilibrium), typically achieved after 48 h of incubation. The kinetics of DOC leaching from frozen peat was studied in batch glass reactors at $1 \text{ g}_{\text{peat}} \text{ L}^{-1}$, 25°C over 132 h of exposure with sampling after 1, 3 and 9 h during first day and after 48, 72 and 132 h the other 5 days. All peat leaching experiments were conducted in replicates, in two parallel reactors. At each sampling, the whole reactor was sacrificed.

2.3. DOC release from and adsorption onto mineral horizons

Three fine sand horizons (E, Bs and Bh exhibiting different concentrations of Fe, Al and C_{org}) from the discontinuous permafrost zone and one silt loamy horizon (Bgh) from the continuous permafrost zone were used for DOC adsorption and release experiments (**Table 1**). The desorption of DOC from Al-Fe-rich sand was studied in 30-mL sterilized glass batch reactors with Milli-Q water, where different amounts of solid phase (0, 0.5, 1, 2, 5, 10, 20 and $100 \text{ g}_{\text{solid}} \text{ L}^{-1}$) were added. The reactors were shaken on a ping-pong shaker at 25°C and the fluid was sampled after 2 days of exposure, filtered through a $0.45 \text{ }\mu\text{m}$ filter unit and stored in the refrigerator for several days prior to analyses. These experiments were run in duplicates, and for each sampling, two entire reactors were sacrificed.

Preliminary DOC adsorption experiments were run in closed (batch) sterilized glass reactors containing 20 ml of peat leachate into which a different amount of mineral fraction (0, 0.02 and 0.2 g) was added. The peat leachate - mineral suspensions were shaken at room temperature over 24 h. These experiments allowed for defining optimal conditions for studying adsorption capacity in dynamic and static experiments. The DOC desorption experiments were also run in dynamic system using two parallel flow-through column reactors, well adapted for both mineral and organic substrates (i.e., Sanderman and Kramer, 2017). For these experiments, we used only the Bh horizon from the discontinuous permafrost zone because

190 this sample contained the highest amount of organic carbon. MilliQ water was delivered from the bottom to
191 the top of a glass column reactor (diameter 1 cm) containing 3 g of mineral phase with a flow rate of
192 $0.05 \pm 0.01 \text{ mL min}^{-1}$. The resulting $0.45 \text{ }\mu\text{m}$ - filtered outlet solution was analyzed each day over the period
193 of 10 days of time and the breakthrough curves of DOC concentration and UV absorbance vs elapsed time
194 were compared between the control run (DOC-free for desorption and mineral-free for adsorption) and the
195 experiment. These dynamic experiments were conducted in duplicates and allowed to constrain the optimal
196 conditions of exposure time and the range of solid and DOC concentration suitable for reliable
197 measurements of adsorption and desorption effects.

198 The main experiments were conducted for each of the 4 mineral horizons listed in **Table 1**, at 1
199 $\text{g}_{\text{mineral soil}} \text{ L}^{-1}$ and 0, 6, 11, 20, 32 and 58 mg DOC L^{-1} concentration of peat leachate, using 30- mL sterile
200 glass bottles that were gently stirred on a ping-pong shaker (100 rpm) at 25°C . After 2 days of exposure
201 time, the supernatant was filtered through a $0.45 \text{ }\mu\text{m}$ disposable filter and stored in the refrigerator for
202 several days before the DOC analyses. For these experiments, we used three independent sub-samples from
203 each soil horizons and each sub-sample was run in duplicates. This provided six identical replicates for each
204 soil horizon. For the sampling, the entire vial was sacrificed.

205 In order to account for the release of ‘native’ DOC when treating the adsorption results, we used the
206 initial mass isotherm approach which is standard in this field (Kaiser et al., 1996; Kothawala et al., 2008;
207 Moore et al., 1992; Nodvin et al., 1986; Ussiri and Johnson, 2004; Vance and David, 1989):

$$208 \quad \text{RE} = m \times [\text{DOC}]_{\text{added}} - b \quad (1)$$

209 where RE is the net DOC sorption (mg C g^{-1}) and b is the amount desorbed to a solution containing no DOC
210 (mg C g^{-1}), corresponding to the release of native soil organic carbon (OC). The $[\text{DOC}]_{\text{added}}$ is the DOC
211 concentration added to the soil suspension (mg C g^{-1}). The empirical partition coefficient m corresponds to
212 the slope of this dependence and represents a fraction of total reactive DOC that is adsorbed by the soil.
213 Further, following Nodvin et al. (1986) and Pengerud et al. (2014), we defined the reactive soil pool (RSP;
214 mg C g^{-1}) as the amount of native soil OC that can readily exchange with DOC in solution under the given
215 experimental conditions as:

$$216 \quad \text{RSP} = b / (1 - m) \quad (2)$$

217

218 2.4. Analyses

219 The DOC was measured in filtered samples using a Shimadzu TOC-VCSN with an uncertainty of 3
220 % and a detection limit of 0.1 mg L⁻¹. The specific UV-absorbance (L mg⁻¹ m⁻¹) was measured in 10 mm
221 quartz cuvette at 254 nm using a CARY-50 UV-VIS spectrophotometer (Bruker, UK) and normalized to the
222 DOC concentration in the sample.

223 The C and N concentrations in dry peat and mineral samples were measured by Cu-O catalysed dry
224 combustion at 900 °C with ≤0.5% precision for standard substances (Thermo Flash 2000 CN Analyzer). The
225 total major composition of mineral fractions (Si, Al, Fe, Ti, S, Na, Ca, Mg, Na, Mn, K, P, O) was measured
226 by X-ray Fluorescence (Bruker AXS GmbH) in tablets of Li borate fused with mineral powder, with an
227 uncertainty of 2% and a detection limit of 0.02% (see **Table S2**). Dithionite-extractable Fe (Fe_d) was
228 measured for bulk soil samples using the method of Mehra and Jackson (1960). Oxalate-extractable Fe (Fe_o)
229 and Al (Al_o) were quantified using standard techniques (van Reeuwijk, 1995). The extracts were measured
230 using flame AAS (Perkin Elmer AAnalyst 300).

231 The BET specific surface area of mineral phases was measured by multi-point N₂ adsorption
232 (Autosorb-1, Quantachrome Instr.). The specific surface area of samples ranged from 0.12 to 2.1 m² g for
233 sands of the discontinuous permafrost zone and amounted to 25.3 m² g for the silt/loam horizon of the
234 continuous permafrost zone. The size of soil particles distribution was assessed using a laser diffraction
235 particle size analyzer (Beckman Coulter, USA). To separate the soil particles into their spherical diameter
236 size classes as following: coarse sand (2-0.50 mm), fine sand (0.50-0.05 mm), silt (0.05-0.002 mm) and clay
237 (<0.002 mm) using the USDA groupings.

238

239 3. Results

240 3.1. Field assessment of C stock in peat and underlying mineral horizons

241 The stock of SOC in peat and mineral horizons at the Khanymey site was estimated from measured C
242 concentrations and bulk density of peat and mineral horizons. We integrated the C pool in mineral horizons
243 located over 100-200 cm under the organic+mineral layer. In the latter, we considered the thickness till the

244 depth where the C concentration dropped down to 0.1 %. The C pool in the discontinuous permafrost zone
245 over 2 m deep on peat mounds encompassed 40 ± 20 cm of the active (thawed) peat layer, 60 ± 20 cm of the
246 frozen peat and 100 cm of the frozen mineral layer (**Fig. 1**). In sands of discontinuous permafrost zone, the
247 OC content decreased from ca. 3% at the top of mineral horizon (0-20 cm) to 0.5-1.5% in the deeper parts of
248 the core (40-80 cm), **Fig. 2A**. The lateral variability of C stock in the 11 sampled sites shown in **Fig. S1** is
249 illustrated in **Table S1**. The average C stock in the peat and mineral deposit was 46.5 ± 22.7 and 14.6 ± 9.2 kg
250 m^{-2} , respectively. It can be seen from this table that the active layer thickness (ALT) and peat thickness have
251 no straightforward impact on C stock in mineral horizons (correlation coefficients are below -0.3, $p > 0.05$).
252 The OC concentration in the silt/loam under peat of the continuous permafrost zone showed a sizeable
253 maximum (6-10%) at 20-40 cm below the peat deposit (**Fig. 2 B**). Overall, the OC pool in 100 cm frozen
254 mineral horizons is generally lower but not negligible compared to the upper 0-100 cm peat layer (**Fig. 2 C**).
255

256 *3.2. Leaching of DOC from frozen peat*

257 Kinetics of DOC leaching from frozen peat demonstrated that stable yield of DOC (5.7 ± 0.5 mg C
258 $\text{g}_{\text{peat}}^{-1}$) is achieved after 48 h of reaction; however, a 70% level of final DOC (4.6 mg C $\text{g}_{\text{peat}}^{-1}$) is reached
259 over first 3 hrs (**Fig. 3A**). The peat-mass normalized DOC concentration (5.7 mg C $\text{g}_{\text{peat}}^{-1}$ at 1 $\text{g}_{\text{peat}} \text{L}^{-1}$) was
260 consistent with the value obtained in batch reactors which were used for preparation of DOC stock solution
261 for adsorption experiments (10 $\text{g}_{\text{peat}} \text{L}^{-1}$ yielded 58 mg L^{-1} of DOC). The 2 day interaction of frozen peat with
262 MilliQ water at different concentrations of peat demonstrated a general decrease in DOC with peat
263 concentration increase from 1 to 20 $\text{g}_{\text{peat}} \text{L}^{-1}$ following an increase at 100 $\text{g}_{\text{peat}} \text{L}^{-1}$ (**Fig. 3B**). Overall, for the
264 range of peat concentrations comparable to those of mineral phases in adsorption experiments (i.e., $1-5$ $\text{g}_{\text{solid}} \text{L}^{-1}$;
265 see section 3.3 below), an average value of 5.5 ± 0.5 mg C $\text{g}_{\text{peat}}^{-1}$ was obtained. The SUVA_{254} also
266 increased from 2.7 to ca. 5.3 $\text{L mg C}^{-1} \text{m}^{-1}$ over 132 h of reaction (**Fig. 3A**), and decreased with peat
267 concentration from 4.2 to 1.7 (**Fig. 3B**).
268

269 *3.3. DOM adsorption onto and leaching from mineral horizons*

270 At low concentrations of added DOC (typically $< 5 \text{ mg L}^{-1}$), all mineral substrates released C with
271 maximal desorption values equal to 0.49 ± 0.23 , 0.13 ± 0.13 , and 0.1 ± 0.1 (mean \pm s.d., $n = 6$) $\text{mg C g}_{\text{soil}}^{-1}$ for
272 Bh, Bs, and E horizons in the discontinuous permafrost zone (**Table 2**). The silt/loam from the continuous
273 permafrost zone (Bgh) exhibited $0.09 \pm 0.02 \text{ mg C g}_{\text{soil}}^{-1}$. Additional desorption experiments were conducted
274 with the Bh horizon (organo-Al-Fe-rich sand) from the discontinuous permafrost zone, at variable soil to
275 water ratios over 48 h of exposure time. These experiments yielded an average value of released OC equaled
276 to $1.20 \pm 0.95 \text{ mg C g}_{\text{soil}}^{-1}$ (for 0.5 to 100 g L^{-1} of sand, $n = 7$, **Fig. 4 A**). The SUVA_{254} of DOM released from
277 the Bh horizon was low at $1 \text{ g}_{\text{sand}} \text{ L}^{-1}$ ($1.2 \text{ L mg C}^{-1} \text{ m}^{-1}$) but raised to approx. $4.9 \text{ L mg C}^{-1} \text{ m}^{-1}$ at higher
278 concentrations of added mineral substrate (2 to $100 \text{ g}_{\text{sand}} \text{ L}^{-1}$).

279 The release of DOC from the Bh horizon was also studied in dynamic mode using a column reactor.
280 The breakthrough curves of DOC and SUVA_{254} demonstrated a contrasting pattern (**Fig. 4 B**). The DOC
281 decreased from ca. $260 \pm 40 \text{ mg L}^{-1}$ to $17 \pm 5 \text{ mg L}^{-1}$ over the first 0-10 h of reaction and was followed by a
282 further decrease to ca. $8\text{-}4 \text{ mg L}^{-1}$ after 100-200 h of leaching. Numerical integration of the breakthrough
283 curve allowed assessing the overall amount of DOC released from 3 g of mineral soil, although insufficient
284 temporal resolution at the beginning of reaction yielded sizable uncertainty. The integral value of DOC
285 released over 200 h of reaction was $2.3 \pm 0.8 \text{ mg C g}_{\text{soil}}^{-1}$, which is somewhat higher than the value obtained
286 in batch (static) reactors ($1.2 \pm 0.6 \text{ mg C g}_{\text{soil}}^{-1}$). An elevated amount of DOC released in dynamic experiments
287 compared to batch reactors could be due to longer (4 x) exposure time of the solid phase in the column-
288 through reactor and enhanced mobilization of internal, strongly bound DOC from poorly accessible pores.
289 Initial SUVA_{254} strongly increased from approx. $0.8 \text{ L mg C}^{-1} \text{ m}^{-1}$ after the first 2 h of reaction to its
290 maximum of $4 \text{ L mg C}^{-1} \text{ m}^{-1}$ after 8 h before gradually decreasing to $1.8 \text{ L mg C}^{-1} \text{ m}^{-1}$ between 10 and 200 h
291 of leaching (**Fig. 4 B**).

292 293 *3.4. Adsorption parameters*

294 A plot of net adsorbed DOC as a function of added DOC concentration demonstrated linear ($R^2 >$
295 0.86 , $p < 0.005$) dependences for both adsorption and desorption parts. The linear regression (Eqn. 1) with

296 $R^2 = 0.86$ to 1.0 ($p < 0.001$) allowed for determination of DOC adsorption parameters (**Fig. 5**). The b and m
297 parameters of Eqn. 1 as well as the RSP value are listed in **Table 2**.

298 The partition coefficient m (Eqn. 1) and the maximal reactive soil pool (RSP, mg C g^{-1}) were highest
299 for the Bs horizon (0.61 ± 0.05 and 0.38 ± 0.02 , respectively; mean \pm s.d., $n = 6$) and lowest for the E horizon
300 (0.17 ± 0.12 and 0.13 ± 0.15 , respectively; mean \pm s.d., $n = 6$). Note quite high uncertainty on adsorption
301 parameters obtained for the E and Bh horizons of the discontinuous permafrost zone. This uncertainty is
302 mostly due to sizable release of DOC from these mineral samples prior the addition of peat leachate. The
303 maximum amount of adsorbed C ranged from 0.15 to $0.63 \text{ mg C g}_{\text{soil}}^{-1}$ when 58 mg C L^{-1} were added;
304 however, no saturation of mineral surface for C was observed (**Fig. 5**). In the discontinuous permafrost zone,
305 maximum adsorption capacities were observed for the Al-Fe-rich sand (Bs horizon) with minimum
306 adsorption capacities observed in poor sand and organo-Al-Fe-rich sand (Bh horizon). The adsorption
307 capacity of the silt/loam horizon from the continuous permafrost zone was intermediate between two sand
308 horizons of the discontinuous permafrost zone. Note that the surface-area normalized adsorption was
309 maximal for the poor sand E horizon ($0.83 \pm 0.42 \text{ mg C m}^{-2}$) of the discontinuous permafrost zone and
310 minimal for the Al-Fe-rich silt/loam (Bgh horizon) of the continuous permafrost zone ($0.01 \pm 0.0004 \text{ mg C m}^{-2}$).
311 Therefore, after normalization to mineral specific surface area, the order of DOC adsorption on mineral
312 horizons was $E > Bs > Bgh$.

313 The evolution of DOC quality which is adsorbed onto/desorbed from mineral horizons was
314 monitored via analysis of the specific ultraviolet absorbance of the aqueous solution. The SUVA_{254} of
315 equilibrium solution exhibited a peculiar pattern depending on the amount of sorbed C (**Fig. 6 A-D**). In the
316 discontinuous permafrost zone, the E horizon exhibited non-systematic variations in SUVA_{254} between 1.5
317 and $6.0 \text{ L mg C}^{-1} \text{ m}^{-1}$. The Bs horizon exhibited an increase in SUVA_{254} with an increase in the amount of
318 adsorbed C varying from 1.5 to $5.0 \text{ L mg C}^{-1} \text{ m}^{-1}$. For the silt/loam Bgh horizon from the continuous
319 permafrost zone, SUVA_{254} slightly increased from 3.3 to 4.4 with an increase in adsorbed C (**Fig. 6 D**).

321 4. Discussion

322 *4.1. Lateral C stock in mineral vs organic layers of WSL peatlands: comparison with other*
323 *estimations in Siberia and across the permafrost zones*

324 The stock of C in peat layer of the permafrost peatbogs of the discontinuous permafrost zone
325 obtained in this study (47 ± 23 kg C m⁻² (mean \pm s.d.); median of 15 kg C m⁻², IQR from 9 to 22 kg C m⁻² over
326 1 m depth, **Fig. 2 C**), is consistent with the range of 31 to 60 kg C m⁻² for this territory (Sheng et al., 2004)
327 and with the value of 44.8 kg C m⁻² provided by Schepaschenko et al. (2013). The Northern Circumpolar
328 Soil Carbon Database lists a value of 44.3 kg C m⁻² for the 0-100 cm layer (Hugelius et al., 2013b).
329 However, if we consider the C in mineral soil horizons (100-200 cm depth), the C stock increases by a factor
330 of 1.4-1.5 and reaches 61 ± 21 kg C m⁻². Similarly, consideration of mineral horizons in the NE European
331 tundra peatlands increased overall C stock by 30% (Pastukhov and Kaverin, 2013) which is similar to our
332 estimations for western Siberia. Note that lack of correlation between peat thickness and C stock in mineral
333 horizons (according to our data, Table S1, section 3.1) suggests that accumulation of C in mineral layers
334 most likely occurs via lateral influx of C-rich shallow subsurface waters such as supra-permafrost waters
335 (Raudina et al., 2018) rather than via direct vertical downward transfer from the peat to the mineral layer.

336 The sizeable stock of OC in mineral horizons of frozen soils of WSL **Fig. 2 C**) is consistent with that
337 reported in Central Siberia (Gentsch et al., 2015a), Northern Siberia (Palmtag et al., 2016), East Siberian
338 Arctic (Gentsch et al., 2015b) and lower than in the yedoma of Eastern Siberia (Hugelius et al., 2013b) and
339 Alaska and Canada (Michaelson et al., 1996; Tarnocai et al., 2009). Although the current estimates of OC
340 stock in WSL comprises more than 2 m depth (70.2 Gt C for WSL, Sheng et al. (2004)) and up to 3 m depth
341 (Hugelius et al., 2014, 2013a), the non-negligible stock of C in the underlying mineral horizon may increase
342 this number by approx. 30 to 50% depending on local peat depth, mineralogical character of mineral
343 deposits, and type of permafrost distribution. In this work, we did not aim to estimate C stock in mineral
344 layers below 3 m depth. In a 7-m deep core from the Tazovsky region (continuous permafrost zone, WSL)
345 that was comprised of 2 m of peat, it was demonstrated that the addition of 4 m of a mineral layer to the first
346 3 m of peat+mineral layer yields an increase in overall SOC stock by only 8.7% (**Fig. S2**). Further, these are
347 silt and clay marine deposits strongly enriched in C compared to the organic-poor sands of the discontinuous
348 permafrost zone. However, given the poor current assessment of C stock in mineral sediments underlying the

349 WSL peat deposits, and the high vulnerability of WSL permafrost with respect to climate warming (i.e., up
350 to 4 m of frozen soils may be thawed over next 50 to 100 years (Vasiliev et al., 2020)), a detailed field-based
351 assessment of OC stocks in mineral layers of this environmentally important region is clearly needed.

352 In this work, we focused exclusively on organic C in peat and mineral horizons. Another important
353 nutrient in the permafrost soils is nitrogen (N). Thus, Meyer et al. (2006) demonstrated that in western
354 Siberia, most of N mineralization occurs in mineral soil horizons rather than in overlaying peat. As such,
355 study of organic N adsorption onto and release from frozen mineral layers in permafrost peatlands should be
356 of high priority.

357 358 *4.2. DOC release from peat and mineral horizons and DOC adsorption capacity*

359 The efficiency of DOC leaching from frozen peat of western Siberia measured in this study (5.5 ± 0.5
360 $\text{mg DOC g}_{\text{peat}}^{-1}$) is very similar to that of the peat from the NE European tundra ($5 \text{ mg DOC g}_{\text{peat}}^{-1}$, Payandi-
361 Rolland et al., 2020) but substantially higher than the values obtained for organic soil samples from Alaska
362 ($0.14\text{-}2.2 \text{ mg g}_{\text{soil}}^{-1}$; Gao et al., 2018). The DOC leaching efficiencies from organic-poor mineral horizons
363 underlying peat deposits of the WSL (0.1 to $0.5 \text{ mg C/g}_{\text{mineral soil}}$) are comparable with those reported for
364 mineral horizons in Canada ($b = 0.05\text{-}0.1 \text{ mg g}^{-1}$, Kothawala et al., 2012) and Norway ($b = 0.17 \pm 0.03 \text{ mg g}^{-1}$,
365 Pengerud et al., 2014).

366 To assess the capacity of mineral horizons to process DOC from the overlaying peat, we present a
367 histogram of soil mass-normalized adsorption/desorption yields (**Fig. 7 A**). Whereas poor sand exhibits
368 comparable adsorption and desorption capacities, Al-Fe-rich sand of the discontinuous permafrost zone and
369 silt/loam of the continuous permafrost zone can adsorb at least 5 times more C than they can release. In
370 contrast, organo-Al-Fe-rich sand of the discontinuous permafrost zone presents the highest desorption
371 capacities. This demonstrates a strong variability of DOC behavior in frozen mineral horizons that underlay
372 peat deposits in western Siberia, and calls a need for a thorough region- and depth-specific inventory of C
373 surface stock depending on underlying mineral deposit type. For example, in the discontinuous permafrost
374 zone, thawing of peat and underlying mineral layers, notable in hollows and depressions, can saturate the
375 mineral horizons in OC originated from peat and plant litter leaching in surface layers. Later, these horizons

376 (such as Bh) are capable of releasing the adsorbed DOC, if the hydrological conditions modify the lateral
377 flow leading to DOC export along the permafrost boundary.

378 At the same time, experiments of this study demonstrate that adsorption of OC on mineral horizons
379 cannot sizably increase SOC stock in these horizons. This increase was only 5 and 15% for the E and Bs
380 horizons of the discontinuous permafrost zone. The Bh horizon exhibited only desorption thus decreasing its
381 stock by 2 %. Overall this indicates the rather stabile non-exchangeable nature of C in these horizons, similar
382 to what is reported for other clay soils (Avneri-Katz et al., 2017). Furthermore, the SUVA₂₅₄ of DOM
383 released from E and Bs horizons was much lower than that of Bh and Bgh horizons (**Fig. 6**). This may
384 reflect more refractory and less labile OM in the Bh and Bgh horizons that contain elevated proportions of
385 clays, Fe, and Al oxides. These compounds are likely to retain aromatic and highly polymerized refractory C
386 (He et al., 2016). Specifically, the long-term persistence of C in subsoil minerals is known to occur due to
387 strong bonds between hydroxylated mineral surfaces and phenolic functional groups of DOM (Kramer et al.,
388 2012).

389 To assess the factors controlling DOC release from and adsorption onto frozen mineral soils we
390 tested a possible link between magnitude of C release/adsorption and basic physical and chemical properties
391 (including Fe and Al content) of study soils. The latter are known to be responsible for DOM adsorption on
392 non-permafrost soils (Kaiser et al., 1996; Karavanova et al., 2020; Nierop et al., 2002). The amount of C
393 desorbed from mineral horizon and the RSP positively correlated ($p < 0.05$) with Al₀, N and C ($r = 0.93$,
394 0.92 , 0.91 , respectively). Maximal adsorption capacity positively correlated ($p < 0.05$) with Fe_d and Fe_o ($r =$
395 0.75 , 0.68 , respectively). Such correlations are consistent with recent observations on strong interactions
396 between iron and organic carbon in European permafrost peatlands (Patzner et al., 2020). At the same time,
397 sizable desorption of DOC from the Bh horizon and high concentration of oxalate-extractable Al for this soil
398 suggest that the majority of Al hydroxides sites are already saturated with organic matter. This strongly
399 corroborates a recent result of Fukumasu et al. (2021) that Al-bearing reactive mineral phases are more
400 important than clay content and Fe-bearing reactive mineral phases for SOC stabilization in topsoils of
401 humid continental climates.

402 It is important to note that the leaching of DOC from the frozen peat and DOC adsorption onto
403 mineral surfaces occur quite fast, within hours to the first day (**Fig. 3A**); a stable DOC concentration in
404 contact with peat is attained within 1-2 days. This is consistent with the generally high reactivity of peat in
405 aqueous solutions (Payandi-Rolland et al., 2020). Similarly, the adsorption pseudo-equilibrium was typically
406 achieved within the first several hours of reaction. This suggests highly labile behavior of OC within the
407 peat-mineral soil profile. As a result, the vertical and lateral water travel rate (from 8 до 80 cm per day,
408 Loiko et al., 2019) rather than chemical reactions of leaching and adsorption will be the limiting step in
409 DOC distribution within the soil profile. Fast reaction of DOC in laboratory experiments of this study further
410 demonstrates that the response of frozen peat and mineral horizons to permafrost thawing will be quasi
411 instantaneous, and that the fast leaching/adsorption reactions may prevent the modification of OC fluxes
412 within the soils- surface waters continuum. It has been shown from incubation experiments that sizeable
413 biodegradation and photo-degradation of DOC in soil and surface waters occurs within 7-40 days (i.e.,
414 Oleinikova et al., 2017b, 2017a; Shirokova et al., 2019; Vonk et al., 2015). In this regard, the temporal
415 variability of DOC sources (leaching from peat or mineral horizons) and sinks (sorption to minerals) will be
416 more important than the autochthonous transformation processes. At the same time, a part of mineral-fixed
417 carbon, especially the labile fraction of DOM, can be decomposed by microorganisms over the time scale of
418 days to month (Panneer Selvam et al., 2017). From the one hand, this may diminish the efficiency of long-
419 term retention of the leached carbon by mineral layers, given quite long (thousands of years) residence time
420 of OM in Siberian soils below 30-50 cm depth (Goryachkin et al., 2000) and very slow rate of DOC
421 movement downward the peat profile (0.047 cm y^{-1} , Zarov et al., 2021). From the other hand, certain mineral
422 horizons, such as clay/silt, are known to stabilize organic matter in soil (Six et al., 2002). Despite the fact
423 that clay/silt soil had a lower capacity to C adsorption compared to Al- and Fe-rich soil (**Fig. 7 A**), this may
424 enhance overall retention ability of C in the soil profile due to lower decomposition rate of OM in the Bgh
425 horizon.

426 *4.3. The impact of C mobility within peat-mineral soil profile at the watershed scale*

427 Climate change in western Siberia is likely to cause a shift of the permafrost boundary northward and
428 an increase in active layer thickness (Anisimov et al., 2013; Frey and Smith, 2003; Pavlov and Moskalenko,

2002; Romanovsky et al., 2010; Vasiliev et al., 2011). According to available scenarios of permafrost thawing in the continuous zone, ALT may reach 1 to 4 m in the western Siberia (Anisimov and Zimov, 2020; Anisimov and Kokorev, 2017) and will inevitably involve currently-frozen mineral horizons into OC release and adsorption. However, these scenarios have to take into account the difference in thawing of micro-landscapes of permafrost peatlands. These include positive (mounds in the discontinuous permafrost zone and polygons in the continuous zone) and negative (hollows/depressions in the discontinuous and cracks in the continuous zone) forms of relief. In the discontinuous permafrost zone, the ALT rarely exceeds 40-50 cm at the mounds and is entirely located within the peat layer. In contrast, the hollows (depressions) are thawed down to the mineral horizons and thus can represent to some extent, an extreme case of the permafrost thawing at mounds in the discontinuous permafrost zone. Based on experimentally-assessed C desorption from mineral horizons, we calculate that thawing of 1 m of frozen sand in the discontinuous permafrost zone may release between 0.05 and 0.5 mg C/g_{soil} m⁻² (**Fig. 7 B**) whereas thawing of frozen silt/loam in the continuous permafrost zone will yield 0.1 mg C/g_{soil} m⁻². Further, the amount of OC originated from leaching of peat that can be adsorbed by unfrozen sand horizons of 1 m thick is between 0.3 and 0.4 kg C m⁻² (**Fig. 7 B**). This is likely to occur in many sites of the discontinuous permafrost zone, where the active layer often extends into the mineral horizon, although it is dependent on the degree of sand coverage by Fe and Al hydroxides. Thus, at the Khanymey site, a transport of OC with seepage into the mineral horizons and the following adsorption onto Al hydroxides of the Bh layer can form organo-mineral spodic horizons.

The values of OC adsorption capacity assessed in this study are non-negligible compared to the amount of DOC that can be leached from peat column by downward migrating fluids (1.38±0.13 kg C m⁻²). This suggests a sizable control by mineral horizons on C migration across the peat - mineral soil profile in the permafrost region. In particular, in the discontinuous permafrost zone, especially at the hollows and depressions, this control is currently visible via release rather than accumulation of DOC in the already saturated Bh horizon. In the continuous permafrost zone, the manifestation of DOC adsorption on mineral layers is anticipated to occur within the next decades.

455 On average, out of $1.38 \pm 0.13 \text{ kg C m}^{-2}$ capable of initial release from the upper 0-100 cm of peat and
456 migrating downwards, $0.25 \pm 0.1 \text{ kg C m}^{-2}$ can be adsorbed in the 100-200 cm underlying Fe- and Al-rich
457 sand and silt with the remaining 1.13 kg C m^{-2} to be exported to lakes and rivers (**Fig. 7 C**). Assuming that,
458 in the continuous permafrost zone, all $200 \pm 100 \text{ cm}$ of frozen peat and underlying sand/silt will thaw over
459 next 100 years, this yields an export potential of $6 \pm 3 \text{ t C km}^{-2} \text{ y}^{-1}$ which is higher than the current estimation
460 of annual DOC export by peatland-draining Siberian rivers (around $3 \text{ t C km}^{-2} \text{ y}^{-1}$, Pokrovsky et al., 2020).
461 The results of this work demonstrate that, in the continuous permafrost zone, on a short-term scale, sizeable
462 amounts of DOC can be liberated to soil waters due to frozen peat thawing and will be quickly captured by
463 underlying mineral horizons if thawing progresses according to the proposed scenarios. In the discontinuous
464 permafrost zone, this OC retention by mineral (Fe- and Al-rich sand horizons) is already occurring in
465 depressions and hollows. Overall, the DOC retention via adsorption can greatly mitigate the “negative
466 “impact of OC release from frozen peat and should be taken into account for modeling of OC transport
467 between soils and rivers in permafrost-bearing landscapes, especially in the continuous permafrost zone
468 where the peat is underlayed by clay/silt horizons, capable of strong DOC adsorption.

470 **Conclusions**

471 We revealed a sizeable stock of organic carbon in mineral horizons underlying peat in the
472 discontinuous and continuous permafrost zone of the western Siberian Lowland (WSL). Significant
473 contributions to the C pool in mineral layer are provided by organo-Al-Fe-rich Bh horizons. These mineral
474 horizons can adsorb part of the C released from peat. The Fe-rich sand of the discontinuous permafrost zone
475 did not exhibit any DOC adsorption but instead released sizable amount of DOC. This horizon contained the
476 highest amount of oxalate extractable Al which could act as strong adsorbent of DOC in the form of Al
477 oxy(hydr)oxides.

478 The on-going climate warming and permafrost thaw will produce a deepening of the active layer into
479 mineral horizons. Such thawing will liberate some amount of DOM from peat and also release of DOM from
480 mineral horizons. However, a sizeable amount of DOC may be retained on mineral horizons via adsorption.
481 This can mitigate the negative impact of climate warming on permafrost thaw and DOC release and thus

attenuate the positive feedback of permafrost thaw on CO₂ emissions. Further measurements of the C pool and adsorption capacity of mineral horizons under frozen peatlands of western Siberia, down to 5-10 m under variable micro-landscapes and biomes (perhaps most importantly under forests), are necessary for improved regional and global modeling of C cycle in permafrost peatlands.

Acknowledgments

Supports from RFBR No 19-29-05209 mk and RFBR 21-54-75001 BF_soils, Belmont Forum project VULCARE grants are acknowledged.

References

- Anisimov, O., Kokorev, V., Zhil'tsova, Y., 2013. Temporal and spatial patterns of modern climatic warming: Case study of Northern Eurasia. *Clim. Change* 118, 871–883. <https://doi.org/10.1007/s10584-013-0697-4>
- Anisimov, O., Zimov, S., 2020. Thawing permafrost and methane emission in Siberia: Synthesis of observations, reanalysis, and predictive modeling. *Ambio* 1–10. <https://doi.org/10.1007/s13280-020-01392-y>
- Anisimov, O.A., Kokorev, V.A., 2017. Russian permafrost in the 21st century: model-based projections and analysis of uncertainties. *Earth's Cryosph. XXI*, 3–9. [https://doi.org/10.21782/ec2541-9994-2017-1\(3-9\)](https://doi.org/10.21782/ec2541-9994-2017-1(3-9))
- Avneri-Katz, S., Young, R.B., McKenna, A.M., Chen, H., Corilo, Y.E., Polubesova, T., Borch, T., Chefetz, B., 2017. Adsorptive fractionation of dissolved organic matter (DOM) by mineral soil: Macroscale approach and molecular insight. *Org. Geochem.* 103, 113–124. <https://doi.org/10.1016/j.orggeochem.2016.11.004>
- Buurman, P., 1985. Carbon/sesquioxide ratios in organic complexes and the transition albic-spodic horizon. *J. Soil Sci.* 36, 255–260. <https://doi.org/10.1111/j.1365-2389.1985.tb00329.x>
- Čapek, P., Diáková, K., Dickopp, J.-E., Bárta, J., Wild, B., Schneckner, J., Alves, R.J.E., Aiglsdorfer, S., Guggenberger, G., Gentsch, N., Hugelius, G., Lashchinsky, N., Gittel, A., Schleper, C., Mikutta, R., Palmtag, J., Shibistova, O., Urich, ., Richter, A., Šantrůčková, H., 2015. The effect of warming on the vulnerability of subducted organic carbon in arctic soils. *Soil Biol. Biochem.* 90, 19-29. DOI: [10.1016/j.soilbio.2015.07.013](https://doi.org/10.1016/j.soilbio.2015.07.013).
- Ciais, P., Tan, J., Wang, X., Roedenbeck, C., Chevallier, F., Piao, S.L., Moriarty, R., Broquet, G., Le Quéré, C., Canadell, J.G., Peng, S., Poulter, B., Liu, Z., Tans, P., 2019. Five decades of northern land carbon uptake revealed by the interhemispheric CO₂ gradient. *Nature*. <https://doi.org/10.1038/s41586-019-1078-6>
- Dahlgren, R.A., Marrett, D.J., 1991. Organic carbon sorption in arctic and subalpine Spodosol B horizons. *Soil Sci. Soc. Am. J.* 55, 1382–1390. <https://doi.org/10.2136/sssaj1991.03615995005500050030x>
- Feng, X., Vonk, J.E., Van Dongen, B.E., Gustafsson, Ö., Semiletov, I.P., Dudarev, O. V., Wang, Z.,

- 520 Montluçon, D.B., Wacker, L., Eglinton, T.I., 2013. Differential mobilization of terrestrial carbon pools
521 in Eurasian Arctic river basins. *Proc. Natl. Acad. Sci. U.S.A.* 110, 14168–14173.
522 <https://doi.org/10.1073/pnas.1307031110>
- 523 Frey, K.E., McClelland, J.W., 2009. Impacts of permafrost degradation on arctic river biogeochemistry.
524 *Hydrol. Process.* 23, 169–182. <https://doi.org/10.1002/hyp.7196>
- 525 Frey, K.E., Smith, L.C., 2003. Recent temperature and precipitation increases in West Siberia and their
526 association with the Arctic Oscillation. *Polar Res.* 22, 287–300. [https://doi.org/10.1111/j.1751-
527 8369.2003.tb00113.x](https://doi.org/10.1111/j.1751-8369.2003.tb00113.x)
- 528 Fukumasu, J., Poepflau, C., Coucheney, E., Jarvis, N., Kloffel, T., Koestel, J., Katterer, T., Svensson, D.N.,
529 Wetterlind, J., Larsbo, M., 2021. Oxalate-extractable aluminum alongside carbon inputs may be a major
530 determinant for organic carbon content in agricultural topsoils in humid continental climate. *Geoderma*,
531 402, Art No 115345.
- 532 Gao, L., Zhou, Z., Reyes, A. V., Guo, L., 2018. Yields and characterization of dissolved organic matter from
533 different aged soils in Northern Alaska. *J. Geophys. Res. Biogeosciences* 123, 2035–2052.
534 <https://doi.org/10.1029/2018JG004408>
- 535 Gentsch, N., Mikutta, R., Alves, R.J.E., Barta, J., Čapek, P., Gittel, A., Hugelius, G., Kuhry, P.,
536 Lashchinskiy, N., Palmtag, J., Richter, A., Šantrůčková, H., Schneckner, J., Shibistova, O., Urich, T.,
537 Wild, B., Guggenberger, G., 2015a. Storage and transformation of organic matter fractions in
538 cryoturbated permafrost soils across the Siberian Arctic. *Biogeosciences* 12, 4525–4542.
539 <https://doi.org/10.5194/bg-12-4525-2015>.
- 540 Gentsch, N., Mikutta, R., Shibistova, O., Wild, B., Schneckner, J., Richter, A., Urich, T., Gittel, A.,
541 Šantrůčková, H., Bárta, J., Lashchinskiy, N., Mueller, C.W., Fuß, R., Guggenberger, G., 2015b.
542 Properties and bioavailability of particulate and mineral-associated organic matter in Arctic permafrost
543 soils, Lower Kolyma Region, Russia. *European J. Soil Sci.*, 66, 722-734. DOI: 10.1111/ejss.12269.
- 544 Groeneveld, M., Catalán, N., Attermeyer, K., Hawkes, J., Einarsdóttir, K., Kothawala, D., Bergquist, J.,
545 Tranvik, L., 2020. Selective adsorption of terrestrial dissolved organic matter to inorganic surfaces
546 along a boreal inland water continuum. *J. Geophys. Res. Biogeosciences* 125, e2019JG005236.
547 <https://doi.org/10.1029/2019JG005236>
- 548 Goryachkin S.V., Cherkinsky A.E., Chichagova O.A., 2000. The soil organic carbon dynamics in high
549 latitudes of Eurasia using ¹⁴C data and the impact of potential climate change. In: R. Lai, J.M. Kimble,
550 B.A. Stewart (eds). *Global Climate and Cold Regions Ecosystems*. Lewis Publishers, p. 145-161.
- 551 Gu, B., Schmitt, J., Chen, Z., Liang, L., McCarthy, J.F., 1994. Adsorption and desorption of natural organic
552 matter on iron oxide: mechanisms and models. *Environ. Sci. Technol.* 28, 38–46.
553 <https://doi.org/10.1021/es00050a007>
- 554 He, W., Chen, M., Schlautman, M.A., Hur, J., 2016. Dynamic exchanges between DOM and POM pools in
555 coastal and inland aquatic ecosystems: A review. *Sci. Total Environ.*
556 <https://doi.org/10.1016/j.scitotenv.2016.02.031>
- 557 Hugelius, G., Bockheim, J.G., Camill, P., Elberling, B., Grosse, G., Harden, J.W., Johnson, K., Jorgenson,
558 T., Koven, C.D., Kuhry, P., Michaelson, G., Mishra, U., Palmtag, J., O'Donnell, J., Schirrmeister, L.,
559 Schuur, E.A.G., Sheng, Y., Smith, L.C., Strauss, J., Yu, Z., 2013a. A new data set for estimating
560 organic carbon storage to 3 m depth in soils of the northern circumpolar permafrost region. *Earth Syst.*
561 *Sci. Data* 5, 393–402. <https://doi.org/10.5194/essd-5-393-2013>
- 562 Hugelius, G., Tarnocai, C., Broll, G., Canadell, J.G., Kuhry, P., Swanson, D.K., 2013b. The northern
563 circumpolar soil carbon database: Spatially distributed datasets of soil coverage and soil carbon storage

- 564 in the northern permafrost regions. *Earth Syst. Sci. Data* 5, 3–13. <https://doi.org/10.5194/essd-5-3-2013>
- 565 Hugelius, G., Strauss, J., Zubrzycki, S., Harden, J.W., Schuur, E.A.G., Ping, C.L., Schirrmeister, L., Grosse,
566 G., Michaelson, G.J., Koven, C.D., O'Donnell, J.A., Elberling, B., Mishra, U., Camill, P., Yu, Z.,
567 Palmtag, J., Kuhry, P., 2014. Estimated stocks of circumpolar permafrost carbon with quantified
568 uncertainty ranges and identified data gaps. *Biogeosciences* 11, 6573–6593. <https://doi.org/10.5194/bg-11-6573-2014>
- 570 Hugelius, G., Loisel, J., Chadburn, S., Jackson, R.B., Jones, M., MacDonald, G., Marushchak, M., Olefeldt,
571 D., Packalen, M., Siewert, M.B., Treat, C., Turetsky, M., Voigt, C., Yu, Z., 2020. Large stocks of
572 peatland carbon and nitrogen are vulnerable to permafrost thaw. *Proc. Natl. Acad. Sci. U. S. A.* 117,
573 20438–20446. <https://doi.org/10.1073/pnas.1916387117>
- 574 IUSS, 2015. International soil classification system for naming soils and creating legends for soil maps,
575 Update 2015. Rome, Italy.
- 576 Jantze, E.J., Lyon, S.W., Destouni, G., 2013. Subsurface release and transport of dissolved carbon in a
577 discontinuous permafrost region. *Hydrol. Earth Syst. Sci.* 17, 3827–3839. <https://doi.org/10.5194/hess-17-3827-2013>
- 579 Jardine, P.M., McCarthy, J.F., Weber, N.L., 1989. Mechanisms of dissolved organic carbon adsorption on
580 soil. *Soil Sci. Soc. Amer. J.* 53(5), 1378-1385,
581 <https://doi.org/10.2136/sssaj1989.03615995005300050013x>
- 582 Kaiser, K., 1998. Fractionation of dissolved organic matter affected by polyvalent metal cations. *Org.*
583 *Geochem.* 28, 849–854. [https://doi.org/10.1016/S0146-6380\(98\)00046-1](https://doi.org/10.1016/S0146-6380(98)00046-1)
- 584 Kaiser, K., Guggenberger, G., 2000. The role of DOM sorption to mineral surfaces in the preservation of
585 organic matter in soils, in: *Organic Geochemistry*. pp. 711–725. [https://doi.org/10.1016/S0146-6380\(00\)00046-2](https://doi.org/10.1016/S0146-6380(00)00046-2)
- 587 Kaiser, K., Guggenberger, G., Zech, W., 1996. Sorption of DOM and DOM fractions to forest soils.
588 *Geoderma* 74, 281–303. [https://doi.org/10.1016/S0016-7061\(96\)00071-7](https://doi.org/10.1016/S0016-7061(96)00071-7)
- 589 Kaiser, K., Zech, W., 1998. Soil dissolved organic matter sorption as influenced by organic and sesquioxide
590 coatings and sorbed sulfate. *Soil Sci. Soc. Am. J.* 62, 129–136.
591 <https://doi.org/10.2136/sssaj1998.03615995006200010017x>
- 592 Kalbitz, K., Schwesig, D., Rethemeyer, J., Matzner, E., 2005. Stabilization of dissolved organic matter by
593 sorption to the mineral soil. *Soil Biol. Biochem.* 37, 1319–1331.
594 <https://doi.org/10.1016/j.soilbio.2004.11.028>
- 595 Karavanova, E.I., Zolovkina, D.F., Stepanov, A.A., 2020. Interaction of the Water-Soluble Organic
596 Substances of Coniferous Litter with Minerals and Horizons of Podzolic Soil and Podzols. *Eurasian*
597 *Soil Sci.* 53, 1234–1246. <https://doi.org/10.1134/S1064229320090070>
- 598 Kawahigashi, M., Kaiser, K., Kalbitz, K., Rodionov, A., Guggenberger, G., 2004. Dissolved organic matter
599 in small streams along a gradient from discontinuous to continuous permafrost. *Glob. Change Biol.* 10,
600 1576–1586. <https://doi.org/10.1111/j.1365-2486.2004.00827.x>
- 601 Kawahigashi, M., Kaiser, K., Rodionov, A., Guggenberger, G., 2006. Sorption of dissolved organic matter
602 by mineral soils of the Siberian forest tundra. *Glob. Change Biol.* 12, 1868-1877.
- 603 Kleber, M., Mikutta, R., Torn, M.S., Jahn, R., 2005. Poorly crystalline mineral phases protect organic matter
604 in acid subsoil horizons. *Eur. J. Soil Sci.* 56(6), 717-725. <https://doi.org/10.1111/j.1365-2389.2005.00706.x>
- 606 Kothawala, D.N., Moore, T.R., Hendershot, W.H., 2009a. Soil properties controlling the adsorption of

- 607 dissolved organic carbon to mineral soils. *Soil Sci. Soc. Am. J.* 73, 1831–1842.
608 <https://doi.org/10.2136/sssaj2008.0254>
- 609 Kothawala, D.N., Moore, T.R., Hendershot, W.H., 2008. Adsorption of dissolved organic carbon to mineral
610 soils: A comparison of four isotherm approaches. *Geoderma* 148, 43–50.
611 <https://doi.org/10.1016/j.geoderma.2008.09.004>
- 612 Kothawala, D.N., Roehm, C., Blodau, C., Moore, T.R., 2012. Selective adsorption of dissolved organic
613 matter to mineral soils. *Geoderma* 189–190, 334–342. <https://doi.org/10.1016/j.geoderma.2012.07.001>
- 614 Kramer, M.G., Chadwick, O.A., 2018. Climate-driven thresholds in reactive mineral retention of soil carbon
615 at the global scale. *Nat. Clim. Chang.* 8, 1104–1108. <https://doi.org/10.1038/s41558-018-0341-4>
- 616 Kramer, M.G., Sanderman, J., Chadwick, O.A., Chorover, J., Vitousek, P.M., 2012. Long-term carbon
617 storage through retention of dissolved aromatic acids by reactive particles in soil. *Glob. Chang. Biol.*
618 18, 2594–2605. <https://doi.org/10.1111/j.1365-2486.2012.02681.x>
- 619 Kremenetski, K. V., Velichko, A.A., Borisova, O.K., MacDonald, G.M., Smith, L.C., Frey, K.E., Orlova,
620 L.A., 2003. Peatlands of the Western Siberian lowlands: Current knowledge on zonation, carbon
621 content and Late Quaternary history. *Quat. Sci. Rev.* 22, 703–723. [https://doi.org/10.1016/S0277-3791\(02\)00196-8](https://doi.org/10.1016/S0277-3791(02)00196-8)
- 623 Loiko, S.V., Raudina, T.V., Lim, A.G., Kuzmina, D.M., Kulizhskiy, S.P., Pokrovsky, O.S., 2019.
624 Microtopography controls of carbon and related elements distribution in the West Siberian frozen bogs.
625 *Geosciences* 9, 291. <https://doi.org/10.3390/geosciences9070291>
- 626 Mehra, O.P., Jackson, M.L., 1960. Iron oxide removal from soils and clay by a dithionite-citrate system
627 buffered with sodium bicarbonate, in: Swineford, A. (Ed.), *Proceedings of the Seventh National*
628 *Conference on Clays and Clay Minerals*. pp. 317–327. <https://doi.org/10.1016/C2013-0-01644-1>
- 629 Meyer, H., Kaiser, C., Biasi, C., Hämmerle, R., Rusalimova, O., Lashchinsky, N., Baranyi, C., Daims, H.,
630 Barsukov, P., Richter, A., 2006. Soil carbon and nitrogen dynamics along a latitudinal transect in
631 Western Siberia, Russia. *Biogeochemistry* 81(2), 239-252.
- 632 Michaelson, G.J., Ping, C.L., Kimble, J.M., 1996. Carbon storage and distribution in tundra soils of Arctic.
633 *Arct. Alp. Res.* 28, 414–424. <https://doi.org/10.1080/00040851.1996.12003194>
- 634 Moore, T.R., de Souza, W., Koprivnjak, J.-F., 1992. Controls on the sorption of dissolved organic carbon by
635 soils. *Soil Sci.* 154.
- 636 Morgalev, Y.N., Lushchaeva, I. V., Morgaleva, T.G., Kolesnichenko, L.G., Loiko, S. V., Krickov, I. V.,
637 Lim, A., Raudina, T. V., Volkova, I.I., Shirokova, L.S., Morgalev, S.Y., Vorobyev, S.N., Kirpotin,
638 S.N., Pokrovsky, O.S., 2017. Bacteria primarily metabolize at the active layer/permafrost border in the
639 peat core from a permafrost region in western Siberia. *Polar Biol.* 40, 1645–1659.
640 <https://doi.org/10.1007/s00300-017-2088-1>.
- 641 Mu, C.C., Zhang, T.J., Zhao, Q., Guo, H., Zhong, W., Su, H., Wu, Q.B., 2016. Soil organic carbon
642 stabilization by iron in permafrost regions of the Qinghai-Tibet Plateau, *Geophys. Res. Lett.*, 43,
643 10,286– 10,294, doi:10.1002/2016GL070071.
- 644 Nierop, K.G.J., Jansen, B., Verstraten, J.M., 2002. Dissolved organic matter, aluminium and iron
645 interactions: Precipitation induced by metal/carbon ratio, pH and competition. *Sci. Total Environ.* 300,
646 201–211. [https://doi.org/10.1016/S0048-9697\(02\)00254-1](https://doi.org/10.1016/S0048-9697(02)00254-1).
- 647 Nodvin, S., Driscoll, C., Likens, G., 1986. Simple partitioning of anions and dissolved organic carbon in a
648 forest soil. *Soil Sci.* 142, 27–35.
- 649 Oleinikova, O. V., Drozdova, O.Y., Lapitskiy, S.A., Demin, V. V., Bychkov, A.Y., Pokrovsky, O.S., 2017a.

- 650 Dissolved organic matter degradation by sunlight coagulates organo-mineral colloids and produces low-
651 molecular weight fraction of metals in boreal humic waters. *Geochim. Cosmochim. Acta* 211, 97–114.
652 <https://doi.org/10.1016/j.gca.2017.05.023>
- 653 Oleinikova, O. V., Shirokova, L.S., Gérard, E., Drozdova, O.Y., Lapitskiy, S.A., Bychkov, A.Y., Pokrovsky,
654 O.S., 2017b. Transformation of organo-ferric peat colloids by a heterotrophic bacterium. *Geochim.*
655 *Cosmochim. Acta* 205, 313–330. <https://doi.org/10.1016/j.gca.2017.02.029>
- 656 Oosterwoud, M. R., Temminghoff, E. J. M., and van der Zee, S. E. A. T. M., 2010. Quantification of DOC
657 concentrations in relation with soil properties of soils in tundra and taiga of Northern European Russia.
658 *Biogeosciences Discuss.*, 7, 3189–3226, <https://doi.org/10.5194/bgd-7-3189-2010>.
- 659 Opfergelt, S., 2020. The next generation of climate model should account for the evolution of mineral-
660 organic interactions with permafrost thaw. *Environ. Res. Lett.* 15, Art No 091003.
661 <https://doi.org/10.1088/1748-9326/ab9a6d>
- 662 Palmtag, J., Ramage, J., Hugelius, G., Gentsch, N., Lashchinskiy, N., Richter, A., Kuhry, P., 2016. Controls
663 on the storage of organic carbon in permafrost soil in northern Siberia. *European J. Soil Sci.*, 67 (4),
664 478–491. DOI: 10.1111/ejss.12357.
- 665 Panneer Selvam, B., Lapierre, J.F., Guillemette, F., Voigt, C., Lamprecht, R.E., Biasi, C., Christensen, T.R.,
666 Martikainen, P.J., Berggren, M., 2017. Degradation potentials of dissolved organic carbon (DOC) from
667 thawed permafrost peat. *Sci. Rep.* 7, Art No 45811. <https://doi.org/10.1038/srep45811>.
- 668 Pastukhov, A. V., Kaverin, D.A., 2013. Soil carbon pools in tundra and taiga ecosystems of northeastern
669 Europe. *Eurasian Soil Sci.* 46, 958–967. <https://doi.org/10.1134/S1064229313070077>
- 670 Patzner, M.S., Mueller, C.W., Malusova, M., Baur, M., Nikeleit, V., Scholten, T., Hoeschen, C., Byrne,
671 J.M., Borch, T., Kappler, A., Bryce, C., 2020. Iron mineral dissolution releases iron and associated
672 organic carbon during permafrost thaw. *Nat. Commun.* 11, 1–11. [https://doi.org/10.1038/s41467-020-](https://doi.org/10.1038/s41467-020-20102-6)
673 20102-6
- 674 Pavlov, A. V., Moskalenko, N.G., 2002. The thermal regime of soils in the north of Western Siberia.
675 *Permafr. Periglac. Process.* 13, 43–51. <https://doi.org/10.1002/ppp.409>
- 676 Payandi-Rolland, D., Shirokova, L.S., Nakhle, P., Tesfa, M., Abdou, A., Causserand, C., Lartiges, B., Rols,
677 J.L., Guérin, F., Bénézeth, P., Pokrovsky, O.S., 2020. Aerobic release and biodegradation of dissolved
678 organic matter from frozen peat: Effects of temperature and heterotrophic bacteria. *Chem. Geol.* 536,
679 119448. <https://doi.org/10.1016/j.chemgeo.2019.119448>
- 680 Pengerud, A., Johnsen, L.K., Mulder, J., Strand, L.T., 2014. Potential adsorption of dissolved organic matter
681 in poorly podzolised, high-latitude soils. *Geoderma* 226–227, 39–46.
682 <https://doi.org/10.1016/j.geoderma.2014.02.027>
- 683 Pokrovsky, O.S., Manasypov, R.M., Kopysov, S.G., Krickov, I.V., Shirokova, L.S., Loiko, S.V., Lim, A.G.,
684 Kolesnichenko, L.G., Vorobyev, S.N., Kirpotin, S.N., 2020. Impact of permafrost thaw and climate
685 warming on riverine export fluxes of carbon, nutrients and metals in Western Siberia. *Water*
686 (Switzerland) 12. <https://doi.org/10.3390/w12061817>
- 687 Pokrovsky, O.S., Manasypov, R.M., Loiko, S., Shirokova, L.S., Krickov, I.A., Pokrovsky, B.G.,
688 Kolesnichenko, L.G., Kopysov, S.G., Zemtsov, V.A., Kulizhsky, S.P., Vorobyev, S.N., Kirpotin, S.N.,
689 2015. Permafrost coverage, watershed area and season control of dissolved carbon and major elements
690 in western Siberian rivers. *Biogeosciences* 12, 6301–6320. <https://doi.org/10.5194/bg-12-6301-2015>
- 691 Porras, R.C., Hicks Pries, C.E., McFarlane, K.J., Hanson, P.J., Torn, M.S., 2017. Association with pedogenic
692 iron and aluminum: effects on soil organic carbon storage and stability in four temperate forest soils.
693 *Biogeochemistry* 133, 333–345. <https://doi.org/10.1007/s10533-017-0337-6>

- 694 Prater, I., Zubrzycki, S., Buegger, F., Zoor-Füllgraff, L. C., Angst, G., Dannenmann, M., Mueller, C. W.
695 2020. From fibrous plant residues to mineral-associated organic carbon - the fate of organic matter in
696 Arctic permafrost soils. *Biogeosciences*, 17, 3367-3383, <https://doi.org/10.5194/bg-17-3367-2020>.
- 697 Prokushkin, A., Gleixner, G., McDowell, W., Ruehlow, S., Schulze, E.D., 2007. Source- and substrate-
698 specific export of dissolved organic matter from permafrost-dominated forested watershed in central
699 Siberia. *Global Biogeochemical Cycles*, 21(4), 10.1029/2007GB002938.
- 700 Raudina, T. V., Loiko, S. V., Lim, A., Manasypov, R.M., Shirokova, L.S., Istigechev, G.I., Kuzmina, D.M.,
701 Kulizhsky, S.P., Vorobyev, S.N., Pokrovsky, O.S., 2018. Permafrost thaw and climate warming may
702 decrease the CO₂, carbon, and metal concentration in peat soil waters of the Western Siberia Lowland.
703 *Sci. Total Environ.* 634, 1004–1023. <https://doi.org/10.1016/j.scitotenv.2018.04.059>
- 704 Raudina, T. V., Loiko, S. V., Lim, A.G., Krickov, I. V., Shirokova, L.S., Istigechev, G.I., Kuzmina, D.M.,
705 Kulizhsky, S.P., Vorobyev, S.N., Pokrovsky, O.S., 2017. Dissolved organic carbon and major and trace
706 elements in peat porewater of sporadic, discontinuous, and continuous permafrost zones of western
707 Siberia. *Biogeosciences* 14, 3561–3584. <https://doi.org/10.5194/bg-14-3561-2017>
- 708 Romanovsky, V.E., Drozdov, D.S., Oberman, N.G., Malkova, G. V., Kholodov, A.L., Marchenko, S.S.,
709 Moskalenko, N.G., Sergeev, D.O., Ukraintseva, N.G., Abramov, A.A., Gilichinsky, D.A., Vasiliev,
710 A.A., 2010. Thermal state of permafrost in Russia. *Permafr. Periglac. Process.* 21, 136–155.
711 <https://doi.org/10.1002/ppp.683>
- 712 Romanovsky, V.E., Kholodov, A.L., Marchenko, S.S., Oberman, N.G., Drozdov, D.S., Malkova, G. V.,
713 Moskalenko, N.G., Vasiliev, A.A., Sergeev, D.O., Zheleznyak, M.N., n.d. Thermal State and Fate of
714 Permafrost in Russia: First Results of IPY.
- 715 Sanderman, J., Kramer, M.G., 2017. Dissolved organic matter retention in volcanic soils with contrasting
716 mineralogy: a column sorption experiment. *Biogeochemistry* 135, 293–306.
717 <https://doi.org/10.1007/s10533-017-0374-1>
- 718 Schepaschenko, D.G., Mukhortova, L. V., Shvidenko, A.Z., Vedrova, E.F., 2013. The pool of organic
719 carbon in the soils of Russia. *Eurasian Soil Sci.* 46, 107–116.
720 <https://doi.org/10.1134/S1064229313020129>
- 721 Schuur, E.A.G., Bockheim, J., Canadell, J.G., Euskirchen, E., Field, C.B., Goryachkin, S. V., Hagemann, S.,
722 Kuhry, P., Lafleur, P.M., Lee, H., Mazhitova, G., Nelson, F.E., Rinke, A., Romanovsky, V.E.,
723 Shiklomanov, N., Tarnocai, C., Venevsky, S., Vogel, J.G., Zimov, S.A., 2008. Vulnerability of
724 permafrost carbon to climate change: Implications for the global carbon cycle. *Bioscience* 58, 701–714.
725 <https://doi.org/10.1641/b580807>
- 726 Schuur, E.A.G., Vogel, J.G., Crummer, K.G., Lee, H., Sickman, J.O., Osterkamp, T.E., 2009. The effect of
727 permafrost thaw on old carbon release and net carbon exchange from tundra. *Nature* 459, 556–559.
728 <https://doi.org/10.1038/nature08031>
- 729 Serikova, S., Pokrovsky, O.S., Ala-Aho, P., Kazantsev, V., Kirpotin, S.N., Kopysov, S.G., Krickov, I. V.,
730 Laudon, H., Manasypov, R.M., Shirokova, L.S., Soulsby, C., Tetzlaff, D., Karlsson, J., 2018. High
731 riverine CO₂ emissions at the permafrost boundary of Western Siberia. *Nat. Geosci.* 11, 825–829.
732 <https://doi.org/10.1038/s41561-018-0218-1>
- 733 Serikova, S., Pokrovsky, O.S., Laudon, H., Krickov, I. V., Lim, A.G., Manasypov, R.M., Karlsson, J., 2019.
734 High carbon emissions from thermokarst lakes of Western Siberia. *Nat. Commun.* 10, Art No 1552,
735 <https://doi.org/10.1038/s41467-019-09592-1>.
- 736 Sheng, Y., Smith, L.C., MacDonald, G.M., Kremenetski, K. V., Frey, K.E., Velichko, A.A., Lee, M.,
737 Beilman, D.W., Dubinin, P., 2004. A high-resolution GIS-based inventory of the west Siberian peat
738 carbon pool. *Global Biogeochem. Cycles* 18. <https://doi.org/10.1029/2003GB002190>.

- 739 Shirokova, L.S., Chupakov, A., Zabelina, S., Neverova, N., Payandi-Rolland, D., Causserand, C., Karlsson,
740 J., Pokrovsky, O.S., 2019. Humic surface waters of frozen peat bogs (permafrost zone) are highly
741 resistant to bio- and photodegradation. *Biogeosciences* 16, 2511–2526. [https://doi.org/10.5194/bg-16-](https://doi.org/10.5194/bg-16-2511-2019)
742 2511-2019
- 743 Schneckner, J., Wild, B., Takriti, M., Eloy Alves, R.J., Gentsch, N., Gittel, A., Hofer, A., Klaus, K., Knoltsch,
744 A., Lashchinskiy, N., Mikutta, R., Richter, A., 2015. Microbial community composition shapes enzyme
745 patterns in topsoil and subsoil horizons along a latitudinal transect in Western Siberia. *Soil Biol.*
746 *Biochem.* 83, 106-115. DOI: 10.1016/j.soilbio.2015.01.016.
- 747 Six, J., Conant, R.T., Paul, E., Paustian, K., 2002. Stabilization mechanisms of soil organic matter:
748 Implications for C-saturation of soils. *Plant and Soil* 241(2), 155-176, DOI:10.1023/A:1016125726789
- 749 Smedberg, E., Mörth, C.-M., Swaney, D.P., Humborg, C., 2006. Modeling hydrology and silicon-carbon
750 interactions in taiga and tundra biomes from a landscape perspective: Implications for global warming
751 feedbacks. *Global Biogeochem. Cycles* 20(2), <https://doi.org/10.1029/2005GB002567>
- 752 Smith, L.C., MacDonald, G.M., Velichko, A.A., Beilman, D.W., Borisova, O.K., Frey, K.E., Kremenetski,
753 K. V., Sheng, Y., 2004. Siberian Peatlands a Net Carbon Sink and Global Methane Source since the
754 Early Holocene. *Science* 303(5656), 353–356. <https://doi.org/10.1126/science.1090553>.
- 755 Tang, J., Yurova, A.Y., Schurgers, G., Miller, P.A., Olin, S., Smith, B., Siewert, M.B., Olefeldt, D., Pilesjö,
756 P., Poska, A., 2018. Drivers of dissolved organic carbon export in a subarctic catchment: Importance of
757 microbial decomposition, sorption-desorption, peatland and lateral flow. *Sci. Total Environ.* 622–623,
758 260–274. <https://doi.org/10.1016/j.scitotenv.2017.11.252>
- 759 Tarnocai, C., Canadell, J.G., Schuur, E.A.G., Kuhry, P., Mazhitova, G., Zimov, S., 2009. Soil organic carbon
760 pools in the northern circumpolar permafrost region. *Global Biogeochem. Cycles* 23, 1–11.
761 <https://doi.org/10.1029/2008GB003327>
- 762 Ussiri, D.A.N., Johnson, C.E., 2004. Sorption of organic carbon fractions by spodosol mineral horizons. *Soil*
763 *Sci. Soc. Am. J.* 68, 253–262. <https://doi.org/10.2136/sssaj2004.2530>
- 764 van Reeuwijk, L.P., 1995. Procedures for soil analysis, Rep. 9, International Soil Reference and Information
765 Centre. Wageningen, The Netherlands.
- 766 Vance, G.F., David, M.B., 1989. Effect of acid treatment on dissolved organic carbon retention by a spodic
767 horizon. *Soil Sci. Soc. Am. J.* 53, 1242–1247.
768 <https://doi.org/10.2136/sssaj1989.03615995005300040042x>
- 769 Vasiliev, A.A., Drozdov, D.S., Gravis, A.G., Malkova, G. V, Nyland, K.E., Streletskiy, D.A., 2020.
770 Permafrost degradation in the Western Russian Arctic. *Environ. Res. Lett.* 15, 045001.
771 <https://doi.org/10.1088/1748-9326/ab6f12>
- 772 Vasiliev, A.A., Streletskaya, I.D., Shirokov, R.S., Oblogov, G.E., 2011. Evolution of cryolithozone of
773 coastal zone of western Yamal during climate change. *Kriosf. Zemli* 2, 56–64.
- 774 Vonk, J.E., Tank, S.E., Bowden, W.B., Laurion, I., Vincent, W.F., Alekseychik, P., Amyot, M., Billet, M.F.,
775 Canário, J., Cory, R.M., Deshpande, B.N., Helbig, M., Jammet, M., Karlsson, J., Larouche, J.,
776 MacMillan, G., Rautio, M., Walter Anthony, K.M., Wickland, K.P., 2015. Reviews and syntheses:
777 Effects of permafrost thaw on Arctic aquatic ecosystems. *Biogeosciences* 12, 7129–7167.
778 <https://doi.org/10.5194/bg-12-7129-2015>
- 779 Zarov, E.A., Lapshina, E.D., Kuhlmann, I., and Schulze, E.-D., 2021. Dissolved organic carbon vertical
780 movement and carbon accumulation in West Siberian peatlands, *Biogeosciences Discuss.* [preprint],
781 <https://doi.org/10.5194/bg-2021-211>, in review.

Table 1. Physico-chemical characteristics and sorption properties of the 4 mineral horizons from the discontinuous (E, Bs and Bh) and continuous (Bgh) permafrost zones.

Soil Horizon	E (n=3)	Bs (n=3)	Bh (n=3)	Bgh (n=3)
Permafrost zone	Discontinuous (Khanymey)			Continuous
Description	poor white sand	poor brunic sand	Al-Fe-rich sand	Silt loam
Material/horizon	albic	brunic	spodic	cryic
pH _{H2O}	5.1±0.4	5.0±0.4	4.9±0.8	5.9±0.7
Sand, %	95	98	82	45
Silt, %	4.3	1.4	16	48
Clay, %	0.7	0.6	2	7
C, mg g ⁻¹	2±1.4	3.8±1.4	32.3±13.5	6.1±1.7
N, mg g ⁻¹	0.12±0.03	0.13±0.05	0.89±0.42	0.2±0.01
Surface area, m ² g	0.12	2.1	1.05	25.3
Total SiO ₂ , %	97±1.2	96±2.1	86±5.1	68.78
Total Al ₂ O ₃ , %	0.8±0.1	1±0.1	3.1±0.5	11.66
Total Fe ₂ O ₃ , %	0.1±0.03	0.2±0.1	0.4±0.1	4.1
Al _{oxalate} , mg g ⁻¹	6.6±3.5	11±5.7	79±29	-
Fe _{oxalate} , mg g ⁻¹	1.41±0.32	1.35±0.22	2.27±0.48	-
Fe _{dithionite} , mg g ⁻¹	2.69±0.94	2.45±0.58	4.86±1.55	-

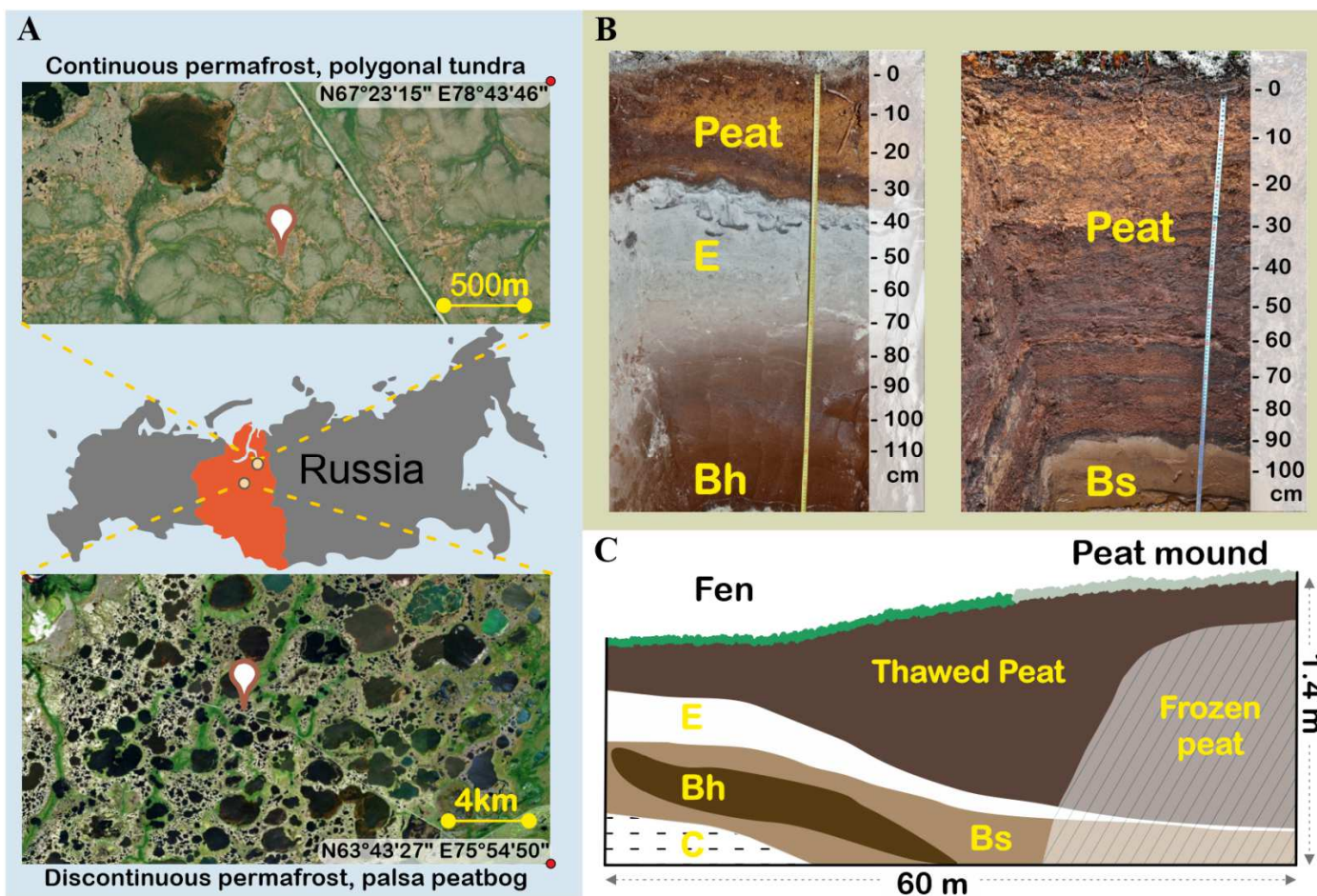
Table 2. Sorption characteristics (Eqn. 1) of the studied mineral horizons.

Soil Horizon	E (n=3)	Bs (n=3)	Bh (n=3)	Bgh (n=3)
Permafrost zone	Discontinuous			Continuous
Adsorbed OC, mg g ⁻¹	0.1±0.05	0.55±0.09	-0.21±0.26	0.35±0.01
Adsorbed OC, mg m ⁻²	0.83±0.41	0.26±0.04	-0.20±0.25	0.014±0.0004
b, mg g ⁻¹ (Desorbed OC)	0.1±0.1	0.13±0.13	0.49±0.23	0.09±0.02
m	0.17±0.12	0.61±0.05	0.2±0.05	0.38±0.02
RSP, mg g ⁻¹	0.13±0.15, y=0.17x-0.12, R ² =0.86	0.37±0.41, y=0.61x-0.14, R ² =1	0.6±0.25, y=0.20x-0.43, R ² =0.69	0.15±0.03, y=0.38x- 0.09, R ² =1

807

808

809



810

811

812

813

814

815 **Fig 1.** Map of the two study sites (A), a photo of soil profiles with peat (used for leachate preparation) and
816 underlying mineral horizons (B), and a schematic representation of soil profile (C).

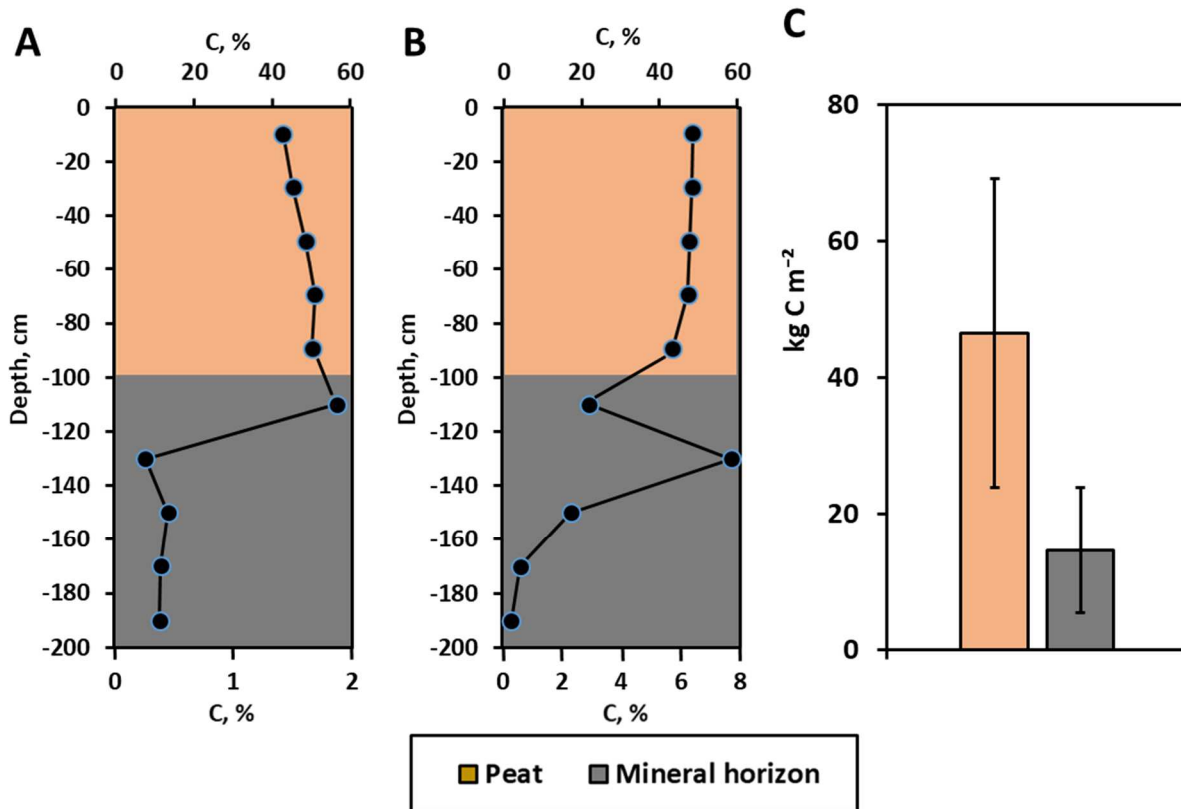


Fig. 2. Examples of depth profile of C concentration in the discontinuous permafrost zone (Khanymey, **A**) and continuous permafrost zone (Tazovsky, **B**) and lateral pools of C in Khanymey, averaged over 11 cores (**C**). Note that C concentration in peat and the mineral part of the core (A and B) are shown in the upper and bottom x-axes, respectively.

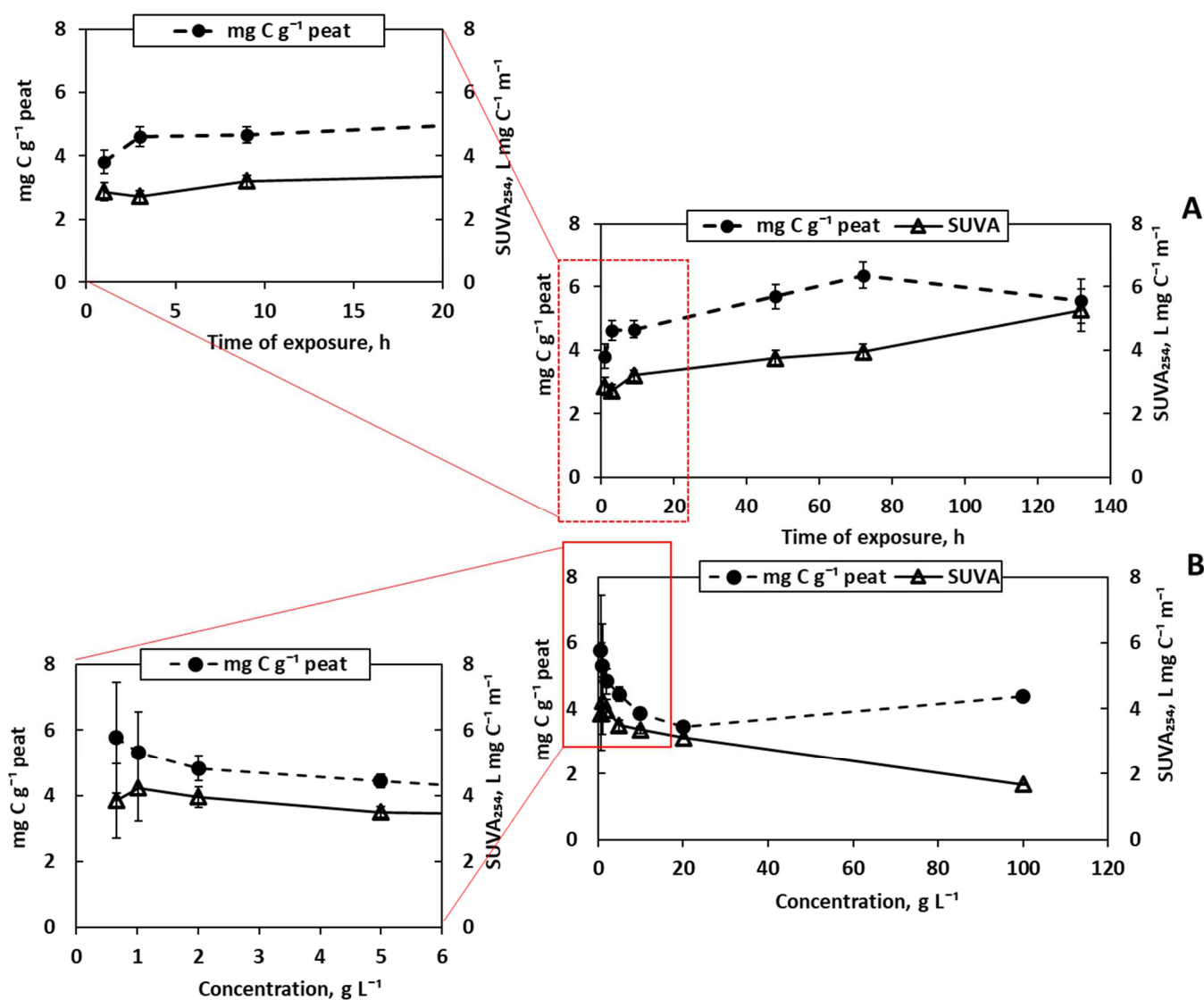


Fig. 3. Patterns of DOC (solid circles and lines, left y-axis) and SUVA₂₅₄ (open triangles and dashed lines, right y-axis) leaching from frozen peat (55-75 cm depth) in batch reactors as a function of exposure time at 1 g peat L⁻¹ (A) and as a function of added peat concentration over 48 h of exposure (B). The error bars represent uncertainties of duplicates unless smaller than symbol size. Inserts illustrate the leaching during short exposure time (top left) and low concentration of peat (bottom left).

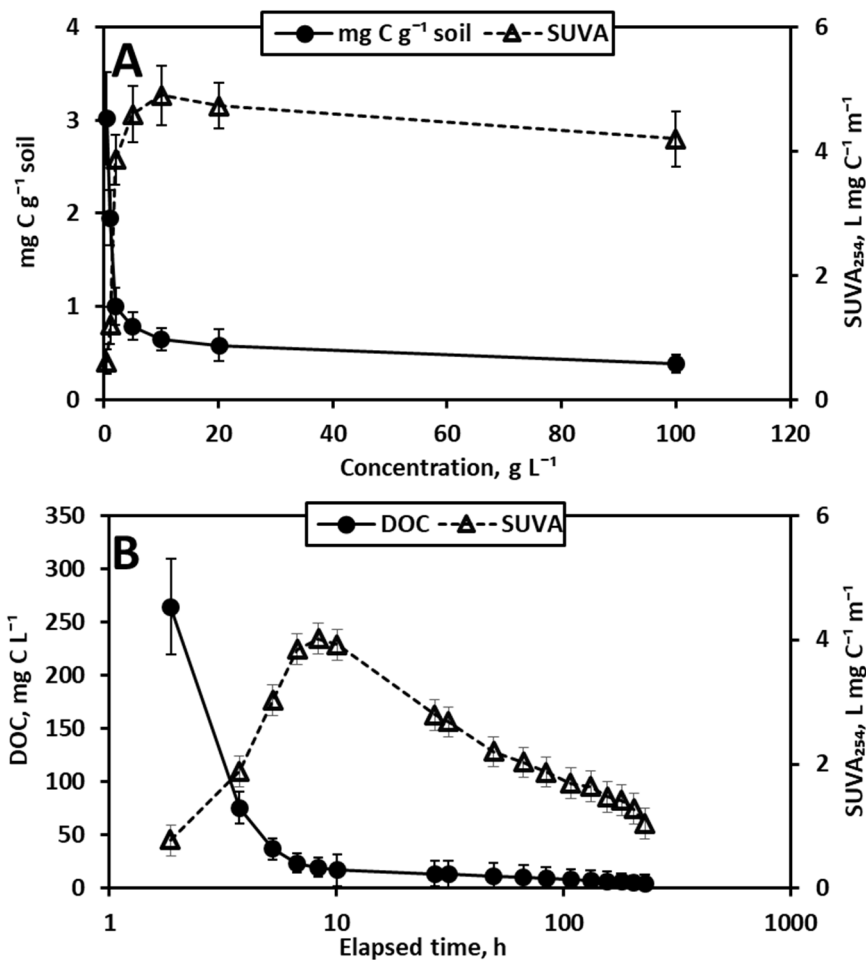


Fig. 4. Leaching of DOM from organo-Al-Fe-rich sand at different concentration of solid phase, after 48 h of equilibration time (A) and the breakthrough curves of DOC in a column reactor filled with 3 g of organo-Al-Fe-rich sand (Bh horizon), with a constant discharge of 3 mL h⁻¹. The error bars represent the uncertainties of duplicates (unless smaller than the symbol size). (B). The evolution of DOC concentration is shown by solid circles and the SUVA₂₅₄ is represented by open triangles and dashed lines. The uncertainties are estimated from the propagation error and analytical procedure.

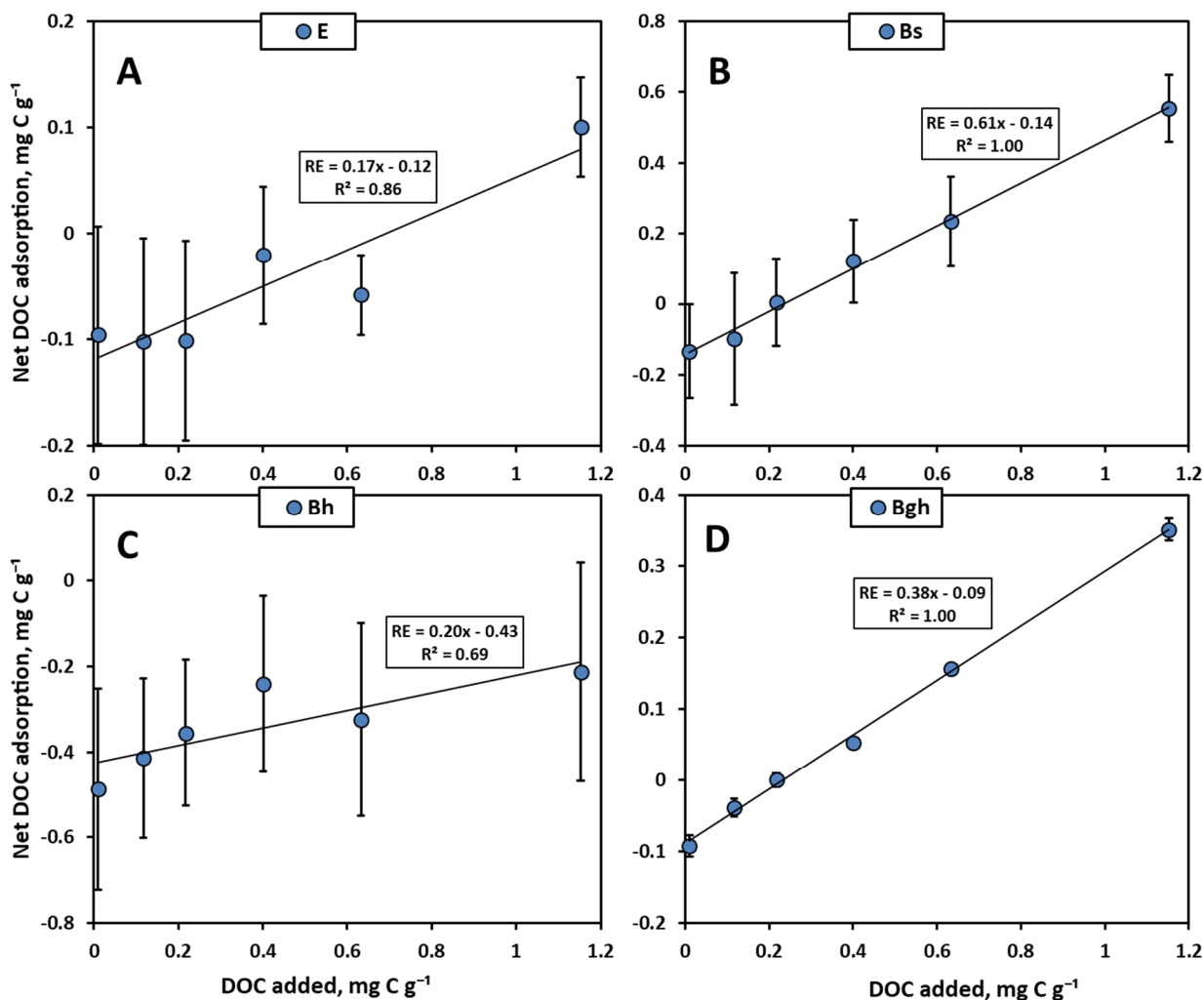


Fig. 5. Amount of DOC adsorbed or desorbed as a function of initial DOC concentration added to the reactor for mineral soil horizons of the discontinuous (A, B, C) and continuous (D) permafrost zone (1 g L^{-1} , 48 h of exposure). The linear regressions represent initial mass isotherms (Eqn. 1). Symbols represent the mean along with s.d. of experimental replicates (2 parallel reactors for 3 subsamples of each soil horizon, $n = 6$). Note that for the Bhg sample, the s.d. are within the symbol size.

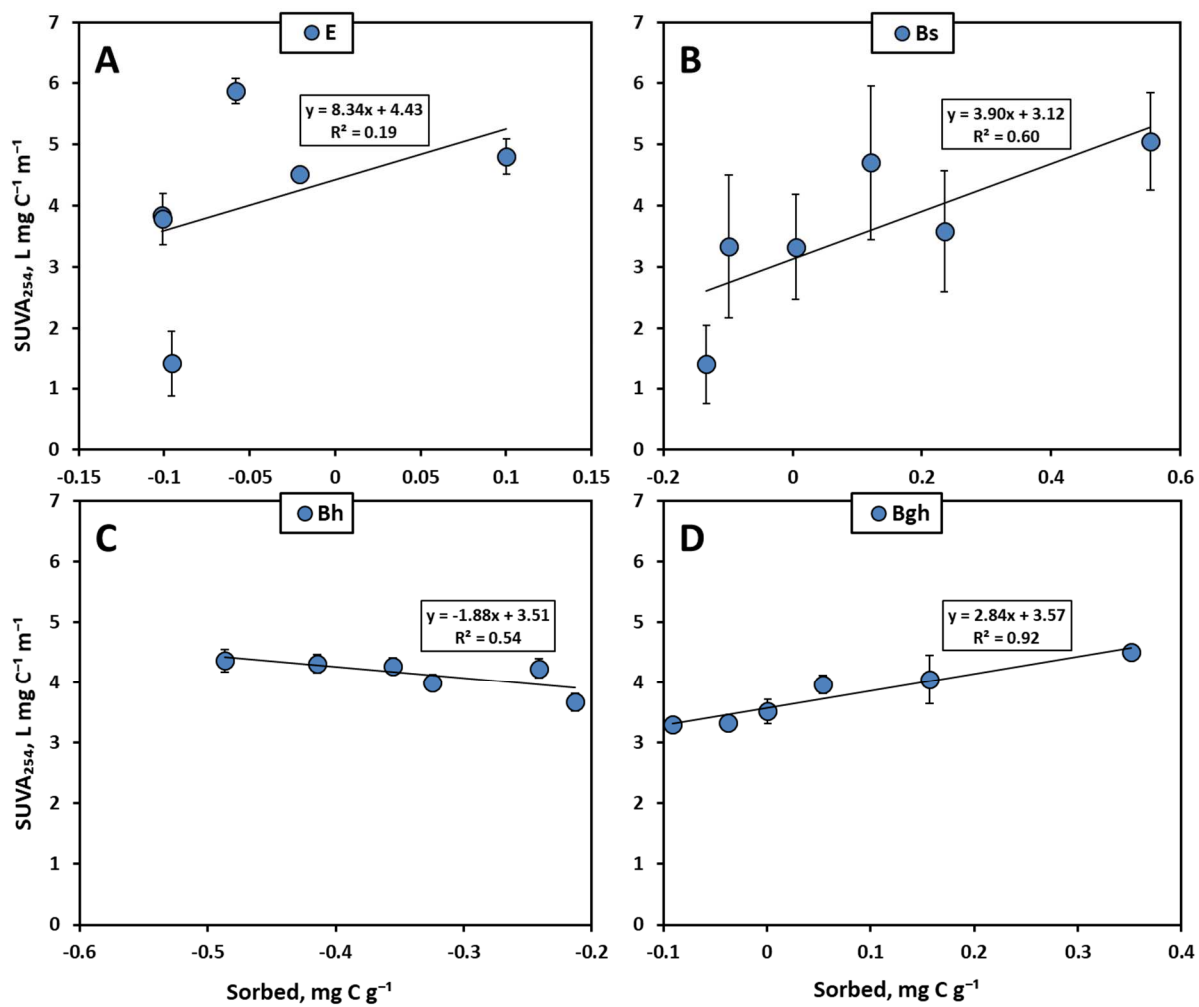


Fig. 6. Evolution of SUVA₂₅₄ (L mg C⁻¹ m⁻¹, mean ± s.d., $n = 6$) as a function of sorbed DOC concentration for mineral soil horizons of the discontinuous (A, B, C) and continuous (D) permafrost zone (1 g L⁻¹ of soil, 48 h exposure time).

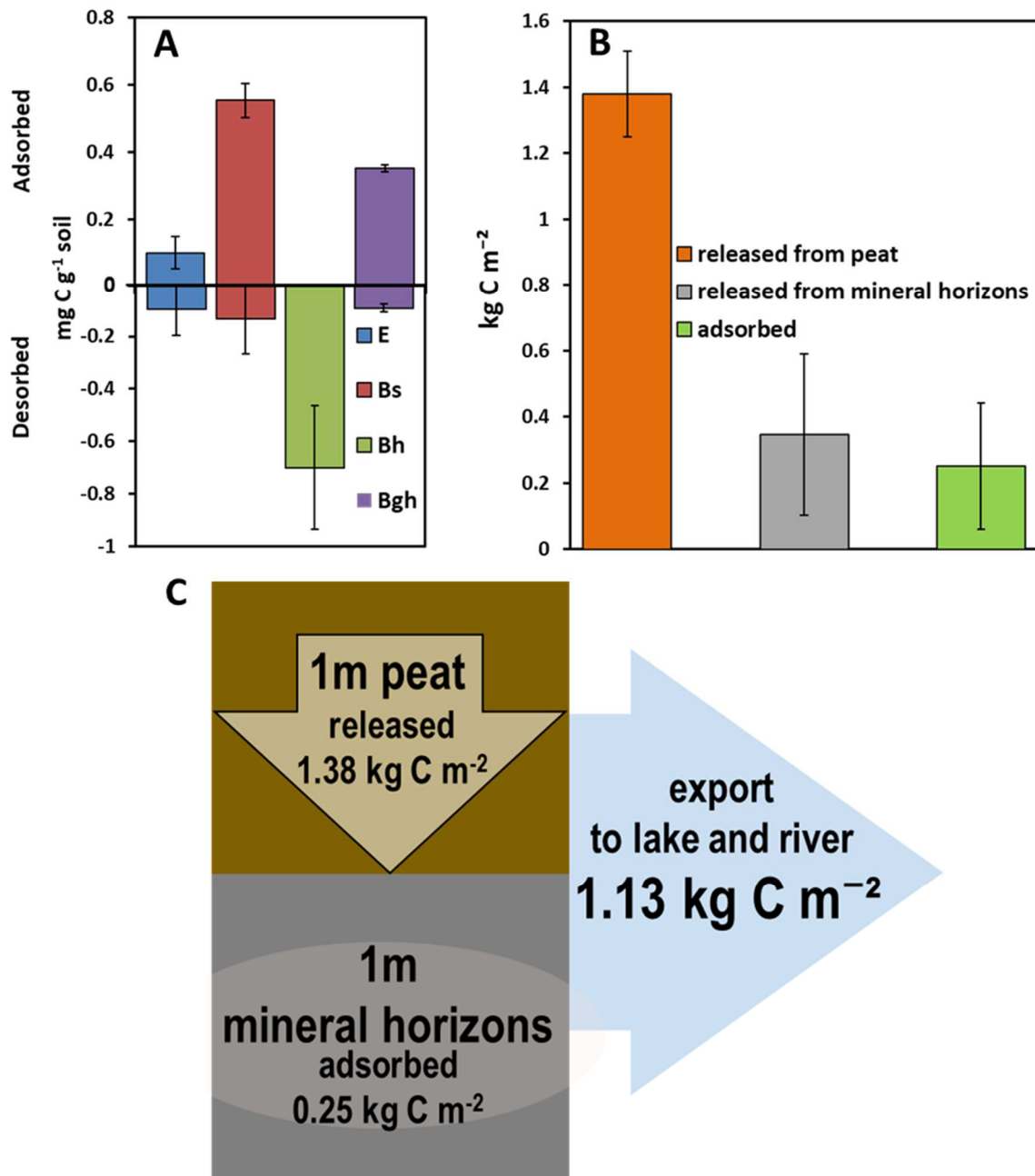


Fig. 7. Soil mass-normalized adsorbed and desorbed C concentration for the 4 mineral horizons (A), the lateral pool of mobile C (over 1 m depth) that can be released from peat, mineral horizons and adsorbed onto minerals (B) and a mass balance illustration of C release from peat, adsorption on mineral horizons and lateral export to hydrological network (C).